สำนักหอสมุดกลาง พระจอมเกล้าลาดกระบัง

Project Final Report

The Impact of Titanate Nanostructure Characteristics on Heat Transfer Enhancement in a Heat Exchanger

Dr. Kunlanan Kiatkittipong

E077893

เลขหมู่..........
เลขทะเบียน 077893
วัน เดือน ปี 22 ก.ย. 2559

b. 12804113
i. ....

This work was financially supported by Revenue Grants 2014

Department of Chemical Engineering, Faculty of Engineering

King Mongkut's Institute of Technology Ladkrabang

This material is reserved for educational use only, not allowed for commercial use.
Forbidden to modify the content, and cite the document when use.

Project title The impact of titanate nanostructure characteristics on heat transfer enhancement in a heat exchanger

Research funding Revenue Grants, Faculty of Engineering, King Mongkut's Institute of Technology Ladkrabang

Project duration 1years from 1 October 2013 to 30 September 2014

Principal investigator Dr. Kunlanan Kiatkittipong

Department of Chemical Engineering, Faculty of Engineering, King Mongkut's Institute of Technology Ladkrabang

Abstract

The aim of this present work is to enhance thermal performance characteristics in a heat exchanger tube by studying: (i) multiple twisted tapes in different arrangements; (ii) TiO2 nanoparticles with different concentrations as the working fluid. The tube inserted the multiple twisted tapes showed superior thermal performance factor when compared with plain tube or the tube inserted a single twisted tape, due to continuous multiple swirling flow and multi-longitudinal vortices flow along the test tube. The higher number of twisted tape inserts led to an enhancement of thermal performance that resulted from increasing contact surface area, residence time, swirl intensity and fluid mixing with multi-longitudinal vortices flow. Moreover, arrangement of twisted tapes in counter current was superior energy saving devices for the practical use, particularly at low Reynolds number. This was especially the case for quadruple counter tapes in the cross directions (CC-QTs) where heat transfer enhancement with relatively low friction loss penalty was deserved. The use of CC-QTs led to the highest thermal performance factor up to 1.45. Using water with TiO2 nanoparticle as a working fluid yielded a higher thermal performance than using pure water. The tube inserted CC-QTs with TiO2/water nanofluid at concentration of 0.21% by volume provided the highest thermal performance factor 1.59, where heat transfer rate and friction factor increased to 3.52 times and 11.7 times of those in the plain tube with water as the working fluid.

Keywords: Heat transfer enhancement , TiO2/water nanofluid, dual/triple/quadruple twisted, heat exchanger

This material is reserved for educational use only, not allowed for commercial use.
Forbidden to modify the content, and cite the document when use.

TABLE OF CONTENTS

This material is reserved for educational use only, not allowed for commercial use.
Forbidden to modify the content, and cite the document when use.

LIST OF TABLES

King Mongkut's Institute of Technology Ladkrabang

This material is reserved for educational use only, not allowed for commercial use.
Forbidden to modify the content, and cite the document when use.

LIST OF FIGURES

This material is reserved for educational use only, not allowed for commercial use.
Forbidden to modify the content, and cite the document when use.

Fig. 14. Contour plots of stream line, velocity vector, turbulent kinetic energy (TKE), temperature fields and local distribution of Nusselt number in the tube fitted with *CC-QTs*: (a) stream line, (b) velocity vector, (c) turbulent kinetic energy (TKE), (d) temperature field and (e) local distribution of Nusselt number.

Fig. 15. Effects of TiO_2 concentration on heat transfer enhancement: (a) Nu and (b) Nu/Nu_p.

Fig. 16. Effects of TiO_2 concentration on friction factor: (a) f and (b) f/f_p.

Fig. 17. Effects of TiO_2 concentration on thermal performance factor.

Fig. 18. Comparisons between predicted data via the empirical correlations and experimental data: (a) Nusselt number, (b) friction factor and (c) thermal performance factor.

King Mongkut's Institute of Technology Ladkrabang

This material is reserved for educational use only, not allowed for commercial use.
Forbidden to modify the content, and cite the document when use.

Chapter 1

Introduction

1.1. Background of the Research

Several heat transfer enhancement (HTE) techniques have been used in many engineering applications such as nuclear reactor, chemical reactor, chemical process, automotive cooling, refrigeration, and heat exchanger, etc. HTE techniques are powerful tools to increase heat transfer rate and thermal performance as well as to reduce of the size of heat transfer system in installing and operating costs. HTE techniques can be classified into 2 categories; (1) active method: by supplying external power source to the fluid or the equipment; (2) passive method: by turbulence promoter (such as special surface geometries, twisted tape, propeller, tangential inlet nozzle, snail entry, axial/radial guide vane, spiral fin) or fluid additives (such as nanofluid), without using any direct external power source. Due to its easy installation/operation and cost saving, passive method has drawn great attention.

One important group of devices used in passive method is swirl flow devices which produce secondary recirculation on the axial flow leading to an increase of tangential and radial turbulent fluctuation. This allows a greater mixing of fluid inside a heat exchanger tube and subsequently reduces a thickness of the boundary layer [1-6]. Among the swirl generators of tube inserts, twisted tapes have gained great attention and widely used for producing compact heat exchangers and upgrading the heat transfer rate of the existing heat exchanger due to its low cost, acceptable thermal performance and ease of manufacture installation [2]. Twisted tapes are generally equipped along the core tube to generate swirl causing the fluid transfer between the core tube and near wall tube. This leads to several mechanisms for heat transfer augmentation by improving flow velocities caused by partial blockage of the tube flow, which directs toward reducing the hydrodynamic or thermal boundary layer thickness. The hydraulic diameter reduction results in greater heat transfer coefficient, lengthening flow path in consequence of a helically twisting fluid consideration has to be taken into account by using twisted tape with a proper geometry motion, improving fluid mixing and thinning thermal boundary layer. However, more pumping power is required when twisted tapes are equipped inside the tube. Therefore, economic consideration has to be taken into account by using twisted tape with a proper geometry.

As nanotechnology has emerged, nanofluid which is the suspensions of nanometer-sized particles or nanoparticles such as TiO2, Al2O3 and CuO are currently attractive for using in heat transfer system as alternative mediums due to their greater thermal conductivities as compared to that of base fluids. The influences of nanofluid

This material is reserved for educational use only, not allowed for commercial use.
Forbidden to modify the content, and cite the document when use.

on heat transfer enhancement were studied by several researchers [50-53]. In general, nanofluid with higher particle loading gave higher heat transfer rate and friction loss. With proper particle loading, most nanofluid yielded appreciable heat transfer enhancement with insignificant friction loss. In addition, nanofluid was utilized together with other heat transfer enhancement devices, especially twisted tapes [54-59]. Apparently, the compound techniques possessed better performance than individual techniques, particularly at high Reynolds number.

1.2. Scope and Objectives

In the light of the aforementioned comments, it has been proven that the heat transfer enhancement by using twisted tape together with nanofluid is a promising approach. However, the influences of the geometries of twisted tape on heat transfer enhancement, friction factor and thermal performance characteristics and nanoparticles are limited explored. To extend the study in the field of heat transfer enhancement by compound technique, this work introduces the use of modified twisted tapes (dual, triple, quadruple twisted tapes) together with TiO2 nanofluid. That is; TiO2 is noncorrosive, environmental friendly and cost effective. The study encompasses Reynolds number from 5400 to 15,200 and TiO2 concentrations from 0.07 to 0.21% by volume.

1.3. Nomenclature

Nomenclature

A	heat transfer surface area, m^2
c_p	specific heat of fluid, $J\ kg^{-1}\ K^{-1}$
D	inside diameter of test tube, m
f	friction factor $= \Delta P/((L/D)(\rho U^2/2))$
h	heat transfer coefficient, $W\ m^{-2}\ K^{-1}$
k	thermal conductivity of fluid, $W\ m^{-1}\ K^{-1}$
L	length of test section, m
$\dot{m}$	mass flow rate, $kg\ s^{-1}$
Nu	Nusselt number $= hD/k$
P	pressure of flow in test tube, Pa
ΔP	pressure drop, Pa
Pr	Prandtl number $= \mu c_p/k$
Q	heat transfer rate, W
q''	heat flux, W/m^2
Re	Reynolds number $= \rho UD/\mu$
t	thickness of the test tube, m
T	temperature, °C
$\tilde{T}$	mean temperature, °C
U	average velocity, $m\ s^{-1}$
V	voltage, V
$\dot{V}$	volume flow rate, $m^3\ s^{-1}$
W	tape width, m
y	pitch length of twisted tape, m
y/W	twist ratio

Greek Symbols

ρ	fluid density, $kg\ m^{-3}$
δ	tape thickness, mm
μ	fluid dynamic viscosity, $kg\ s^{-1}\ m^{-1}$
η	thermal performance factor
ϕ	concentration of nanofluid, % by volume

Subscripts

b	bulk
conv	convection
i	inlet
f	nanofluid
np	nanoparticle
o	outlet
p	plain tube or particle
t	twisted tape
w	wall or water

Abbreviations

ST	single tape as single swirl flow generator
Co-DTs	dual co-tapes as co-dual swirl flow generators
C-DTs	dual counter tapes as counter-dual swirl flow generators
Co-TTs	triple co-tapes as co-triple swirl flow generators
Co-QTs	quadruple co-tapes as co-quadruple swirl flow generators
CC-QTs	quadruple counter tapes as counter-quadruple swirl flow generators
PC-QTs	quadruple counter tapes as parallel-quadruple swirl flow generators

This material is reserved for educational use only, not allowed for commercial use.
Forbidden to modify the content, and cite the document when use.

Chapter 2

Theory and Literature Review

2.1. Theory

2.1.1. Mathematical model and numerical method

The numerical model for fluid flow and heat transfer in a circular tube fitted with single/dual/triple/quadruple twisted tapes with different tape arrangements was developed under the following assumptions: steady, three-dimensional and turbulent incompressible fluid flow. Body forces, radiation heat transfer and viscous dissipation are ignored. Based on the above assumptions, the tube flow is governed by the continuity, the Navier-Stokes equations and the energy equation. The energy equation was discretized by the QUICK scheme while the other governing equations were discretized by the second-order upwind numerical scheme, decoupling with the SIMPLE algorithm and solved using a finite volume approach. The solutions were considered to be converged when the normalized residual values were less than 10^{-9} for energy equation and less than 10^{-5} for other governing equations. More details of the numerical method and parameter conditions can be found in Table 3.

2.1.2. Data reduction

The thermophysical properties (density, specific heat, viscosity and thermal conductivity) of TiO_2/water nanofluid were evaluated based on the properties of the base fluid and nanoparticles. It was assumed that nanoparticles were well dispersed in the base fluid (water). Although this assumption may be not true in real systems because of some physical phenomena such as particle migration, it is acceptable for evaluating the approximate physical properties of nanofluids. All properties of nanofluid depend on nanoparticle volume concentration (ϕ) as shown below.

The density and specific heat of nanofluid were evaluated from equation (1) and (2), respectively.

$$\rho_{nf} = (1-\phi)\rho_w + \phi\rho_{np} \tag{1}$$

$$c_{p,nf} = \frac{\phi\rho_{np}c_{p,np} + (1-\phi)\rho_w c_{p,w}}{\rho_{nf}} \tag{2}$$

These equations were appropriate for nanofluid through experimental validation by Pak and Cho [60] and Xuan and Roetzel [61].

This material is reserved for educational use only, not allowed for commercial use.
Forbidden to modify the content, and cite the document when use.

The thermal conductivity was calculated from Maxwell model [62] as shown in Eq. (3) which is recommended for homogeneous and low volume concentration liquid-solid suspensions with randomly dispersed, uniformly sized and non interacting particles [63].

$$\frac{k_{nf}}{k_w}=\frac{k_{np}+2k_w+2\phi(k_{np}-k_w)}{k_{np}+2k_w-\phi(k_{np}-k_w)} \tag{3}$$

Viscosity of nanofluid was calculated via the general Einstein's formula [64].

$$\mu_{nf}=\mu_w(1+\eta\phi) \tag{4}$$

Where $\eta = 2.5$, as recommended for hard particles [63].

2.1.3. Heat transfer and friction factor measurements

The steady state convective heat transfer rate was assumed to be equal to the heat transfer to the working fluid in the test tube as expressed below.

$$Q_f = Q_{conv} \tag{5}$$

where

$$Q_f = \dot{m}c_{p,f}(T_o - T_i) = VI - Q_{loss} \tag{6}$$

The heat absorbed by water at thermal equilibrium was found to be 3-7% lower than that supplied by electrical heater plates. This is due to convection and radiation heat losses from the test tube to surroundings. Thus, only the heat transfer rate absorbed by fluid was taken for internal convective heat transfer coefficient calculation. The convection heat transfer from the test tube can be written by

$$Q_{conv} = hA(\tilde{T}_w - T_b) \tag{7}$$

where

$$T_b = (T_o + T_i)/2 \tag{8}$$

and

$$\tilde{T}_w = \sum T_w / 15 \tag{9}$$

where the average wall temperature ($\tilde{T}_w$) was calculated from 15 data of the local wall temperatures (T_w) lined between the inlet and the exit of the test tube. The average heat transfer coefficient (*h*) and the average Nusselt number (*Nu*) were then estimated as follows:

$$h = \dot{m}c_{p,f}(T_o - T_i) / A(\tilde{T}_w - T_b) \tag{10}$$

$$Nu = hD/k \tag{11}$$

This material is reserved for educational use only, not allowed for commercial use.
Forbidden to modify the content, and cite the document when use.

In the experiment, the local mean bulk temperatures of the fluid (*f*) flowing into the test section were determined from $T_{bx} = T_{bi} + \dot{q}\pi DL_x / \dot{m}c_{p,f}$. The local and mean heat transfer coefficients were calculated from

$h_x = \dot{q} / (T_{wx} - T_{bx})$

where $\dot{q}$ is a heat flux.

The Reynolds number is given by

$$\mathrm{Re} = UD / \nu \tag{12}$$

Friction factor was evaluated pressure drop within the system as

$$f = \frac{\Delta P}{(L/D)\rho U^2/2} \tag{13}$$

where U is mean water velocity in the tube. All of thermo-physical properties of a fluid was determined based on the overall bulk water temperature achieved from Eq. (8).

The thermal performance factors of the tube equipped with single/dual/triple/quadruple twisted tapes were evaluated under constant pumping criterion. The constant pumping power criterion can be expressed as

$$\left(\dot{V}\Delta P\right)_p = \left(\dot{V}\Delta P\right)_t \tag{14}$$

Under the criterion, the relationship between friction and Reynolds number can be expressed as:

$$\left(f\,\mathrm{Re}^3\right)_p = \left(f\,\mathrm{Re}^3\right)_t \tag{15}$$

$$\mathrm{Re}_p = \mathrm{Re}_t \left(f_t/f_p\right)^{1/3} \tag{16}$$

As preliminary design guidance to the selection of a technique, the thermal performance factor can be evaluated based on the power consumption per unit mass of fluid. The thermal performance factor, η is defined as the ratio between the heat transfer coefficient for the tube with heat transfer promoter (h_t) and the value for the plain tube (h_p) at identical pumping power.

$$\eta = \left.\frac{h_t}{h_p}\right|_{pp=} \left.\frac{Nu_t}{Nu_p}\right|_{pp=} \left(\frac{Nu_t}{Nu_p}\right)\left(\frac{f_t}{f_p}\right)^{-1/3} \tag{17}$$

where Nu_t and Nu_p, are respectively, Nusselt number for tube with twisted tape inserts and plain tube while f_t and f_p, are respectively, friction factor for tube with twisted tape inserts and plain tube.

This material is reserved for educational use only, not allowed for commercial use.
Forbidden to modify the content, and cite the document when use.

2.2. Literature Reviews

Since Whitham et al. [1] reported the success of using twisted tapes in improving heat transfer in heat exchanger, heat transfer enhancement using the devices have been extensively studied. In particular, the modifications of twisted tape have been continually released. Recently, many research groups modified various types of twisted tapes. They found that the geometries of twisted tapes have significant influences on fluid mixing and heat transfer rate [7-24]. The modified edges or center of twisted tapes have been proposed to induce stronger turbulence intensity in the vicinity of tube wall or the core of tube. Rahimi et al. [25] numerically evaluated heat transfer enhancement by modified twisted tapes including jagged perforated and notch twisted tapes. Their results revealed that among the studied twisted tapes, jagged twisted tape possessed the best performance with 31% higher heat transfer rate and 22% higher thermal performance factor compared to those of typical twisted tape. Sivashanmugam and Suresh [26-29] compared the heat performance and pressure drop of full length helical twisted and the helical twisted with spacer length in laminar and turbulent flow region, and found that the tape with spacer length within 10% of the entire length could preserve heat transfer augmentation and decrease pressure drop simultaneously. Krishna et al. [30] reported that the twisted tape with twist ratio of 4 and width of 1 inch provided an appreciable heat transfer enhancement when space length was kept below 2 inches. The experimental results reported by Sivashanmugam et al. [31,32] showed that right-left helical screw inserts exhibited a superior heat transfer enhancement to straight helical twist at the same twist ratio. Later, the helical and left-right twisted tapes were used in thermosyphon solar water heating system to enhance heat transfer and thermal performance [33]. Moreover, Nagarajan et al. [34] reported that the geometries of left-right twisted tapes played an important role in governing heat transfer, friction factor and thermal performance. Jaisankar et al. [35] employed typical twisted tapes with different twist ratios (3.0-5.0) in a solar water heater, and found that the tape with a smaller twist ratio provided higher heat transfer enhancement as well as friction factor due to a stronger swirl flow intensity.

Murugesan et al. [36] employed twisted tape used in conjunction with the wire nails, namely WN-TT in a double pipe heat exchanger. As compared to typical twisted tape (TT), WN-TT offered a higher heat transfer rate, friction factor and thermal performance factor, attributed to extra turbulent flows. In addition, Murugesan et al. [37, 38] invented V-cut and trapezoidal-cut twisted tape inserts for comparison with a typical twisted tape. It was found that V-cut and trapezoidal-cut twisted tape inserts induced a common swirl flow coupled with an extra fluid disturbance and secondary flow in the vicinity of the tube wall, resulting in superior heat transfer enhancement as compared to common swirl flow associated by the use of the typical twisted tape (TT).

This material is reserved for educational use only, not allowed for commercial use.
Forbidden to modify the content, and cite the document when use.

Saha's research group [39-42] investigated the friction factor and heat transfer for laminar flow through a circular duct having integral helical-rib-roughness/axial-corrugation and fitted with center-cleared twisted tape. They found that the compound device gave much better heat transfer enhancement than the individual technique acting alone.

Eiamsa-ard et al. [43] investigated the effect of coupling twisted tapes on heat transfer enhancement in a heat exchanger. The studied parameters were: (i) twisted tape orientation; co twisted tapes (co-CTTs) and counter twisted tapes (counter-CTTs); (ii) width ratio; (iii) twist ratio. The experimental results revealed that heat transfer, friction loss and thermal performance factor increased with decreasing twist ratio and increasing width ratio. Moreover, Eiamsa-ard et al. [44] studied the effect of twin deltawinged twisted tapes and their arrangements on heat transfer, pressure drop and thermal performance characteristics of a heat exchanger tube. Three different arrangements were determined: (1) the wing-tips pointing upstream of the flow (TTW-up, twin delta-winged twisted tape in counter-flow arrangement) (2) the wing-tips pointing downstream of the flow (TTW-down, twin delta-winged twisted tape in co-flow arrangement) and (3) the wing-tips pointing opposite direction (TTW-o, opposite winged twisted tape). At similar conditions, TTW-up gave the highest Nusselt number, friction factor and thermal performance factor, followed by TTW-o and TTW-down. The TTW-up with wing-tip angle of 20_ gave the maximum thermal performance factor of 1.26 along with the Nusselt number and friction factor of 2.57 and 8.55 times compared to those of the plain tube.

Chang et al. [45] examined the heat transfer and pressure drop characteristics in a tube fitted with single, twin and triple twisted tapes in a heat exchanger tube. Among the tested tapes, the triple twisted tapes offered the highest heat transfer rate and thermal performance factor. Eiamsa-ard et al. [46] determined the effect of the twin counter/co twisted tapes (counter/co-swirl tape) on the thermohydraulic performance in a heat exchanger tube. The twin counter twisted tapes (CTs) were used as the counter-swirl flow generators while twin co twisted tapes (CoTs) were used as co-swirl flow generators. The heat transfer rates for the tube fitted with the CTs were 12.5e44.5% and 17.8e50% higher than those with the CoTs and typical twisted tape, respectively. Eiamsa-ard et al. [47] also investigated heat transfer and pressure loss by insertion of regularly-spaced twin/dual twisted tapes in a round tube with three different space ratios (s/D , 0.75, 1.5 and 2.25). Evidently, the tape with smallest space ratio of 0.75, gave the highest heat transfer rate which was 140% higher than that of plain tube. Zhang et al. [48] studied the heat transfer enhancement in the tube fitted with triple and quadruple twisted tapes. The simulation was conducted in order to gain an understanding of physical behavior of the thermal and fluid flow in the tube fitted with triple and

This material is reserved for educational use only, not allowed for commercial use.
Forbidden to modify the content, and cite the document when use.

This material is reserved for educational use only, not allowed for commercial use.
Forbidden to modify the content, and cite the document when use.

quadruple twisted tapes. They found that Nusselt number increased up to 171% and 182% by using triple and quadruple twisted tapes as compared to that in the plain tube. Hong et al. [49] presented a 3D numerical simulation of turbulent heat transfer and flow characteristics in converging-diverging tubes (CDs) and converging-diverging tubes equipped with twin counter-swirling twisted tapes (C-DTs). Their results revealed that geometric parameters played important role on the thermal performance.

This material is reserved for educational use only, not allowed for commercial use.
Forbidden to modify the content, and cite the document when use.

Chapter 3

Experimental Strategy

3.1. Twisted tapes

The schematic view and details of the single, dual, triple and quadruple twisted tapes with different arrangements are shown in Fig. 1 and Table 1. All twisted tapes were made of aluminum strip with a thickness of 0.8 mm, which is a minimum twisting operation, and a length of 1000 mm. To fabricate a twisted tape, one end of a straight tape was clamped while another end was carefully twisted to achieve a desired twist length. Single twisted tape was 18 mm in width while dual, triple and quadruple twisted tapes were 8 mm in width. The tapes were formulated at constant twist ratio (y/W) of 3 where twist ratio is defined as twist length (180°/twist length) to tape width (W). For dual, triple and quadruple twisted tapes, each tape was individually twisted and subsequently welded together using special glue. In the experiment, the swirl direction swirl corresponding to tape arrangement was designed as: i) co-swirl flow; all tapes were aligned to be twisted in the same direction. In this case, dual, triple and quadruple twisted tapes were assigned as *Co-DTs/Co-TTs/Co-QTs*, respectively, ii) counter-swirl flow; this arrangement was designed for dual and quadruple twisted tapes. In the case of dual twisted tapes, two tapes were aligned to be twisted in opposite directions and assigned as *C-DTs*. In the case of quadruple twisted tapes, two tapes were aligned to be twisted in the same direction which was opposite to that of other two tapes. In addition, the quadruple counter tapes consisting of two pairs of tapes were in two different arrangements, to produce (1) parallel counter-swirl flow and (2) cross counter-swirl flow. For parallel counter-swirl flow, the tapes in each pair produced swirl flow in the same direction; in this case the quadruple counter tapes were assigned as *PC-QTs*. For cross counter-swirl flow, the tapes in each pair produced swirl flow in the opposite directions. The quadruple counter tapes were assigned as *CC-QTs*.

This material is reserved for educational use only, not allowed for commercial use.
Forbidden to modify the content, and cite the document when use.

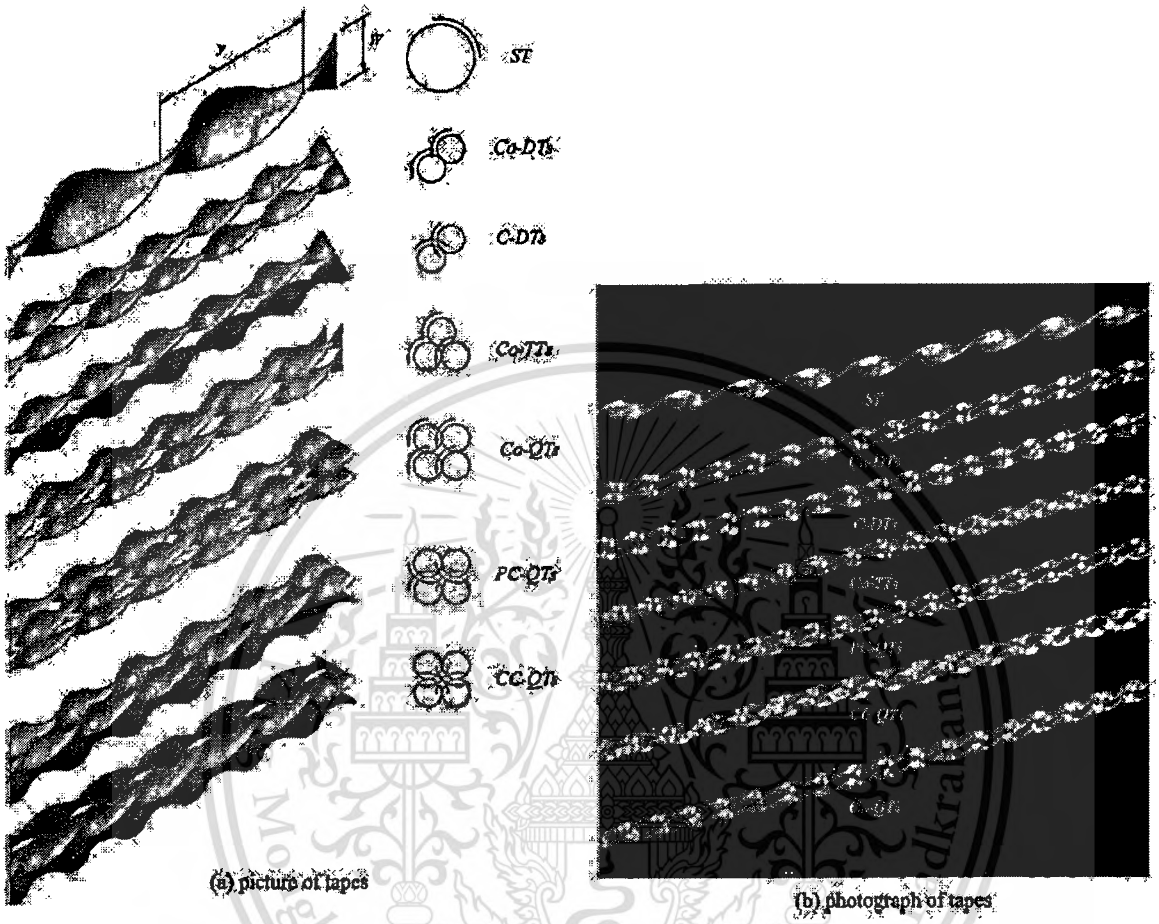

Fig. 1. Picture view and photograph of the dual/triple/quadruple twisted tapes with different tape arrangements: (a) picture of tapes and (b) photograph of tapes.

3.2. Preparation and characterization of nanofluid

Anatase TiO2 nanoparticles, with an average diameter of 15 nm were purchased from Nanostructured and Amorphous Material, Inc, USA. The macro photograph of nanoparticles (TiO2) is shown in Fig. 2a. Closer inspection of morphology was analyzed by a scanning electron microscope (SEM) in Fig. 2b. Pure anatase TiO2 nanoparticles were confirmed by X-ray Diffraction (XRD) spectra (Fig. 2c). To prepare nanofluid, TiO2 nanoparticles were dispersed into 800 mL of de-ionized water used as the base liquid. Then, the mixture was

This material is reserved for educational use only, not allowed for commercial use.
Forbidden to modify the content, and cite the document when use.

sonicated continuously for 180 min in an ultrasonic bath under ultrasonic pulses of 100 W at 36 ± 3 kHz for proper dispersion. Fig. 2d demonstrates that sonicated nanofluid is homogenous than non-sonicated nanofluid.
Moreover, the sonication treatment significantly improved the stability of suspension. As observed, the TiO2 nanoparticles would precipitate over 180 min. This is, TiO2 nanoparticles are still stable in water before feeding into the tube. Nanofluid was prepared at three different TiO2 concentrations of 0.07%, 0.14% and 0.21% by volume..

3.3. Experimental set-up and procedure

The apparatus with the basic components and fluid flow system are presented in Fig. 3. The test rig consists of a 7.5 tons water chiller (Carrier), water tank, data logger for collecting experimental data, rotameter meter to measure a volumetric water flow rate and a heat transfer test section. The test tube was made of copper tube with an inner diameter of 19mm (D), an outer diameter of 22 mm, a wall thickness of 1.5 mm (t), and a length of 1000 mm (L). The rather long tube provided sufficient contact surface between the tapes and tube wall for the firm attachment of the tapes to the tube without the need of any extra fitting. The tube was wound with electrical heating wire covered with ceramic beads. During the test, the tube was heated by continually winding flexible electrical wire, providing a uniform heat flux condition. The electrical output power was controlled by a variac transformer to achieve a constant heat flux condition along the entire length of the test section by keeping the current less than 10 A. The outer surface of the test tube was well insulated to minimize convective heat losses to surroundings. In the experiment, the heat transfer losses from the test tube were found to be around 3e7% of the total heat input ($Q \approx IV$). The inlet and outlet temperatures of the bulk water were measured by a multi-channel temperature measurement unit in conjunction with the resistance temperature detectors (RTDs). Four thermocouples were placed at 1000 mm upstream and 50 mm downstream of the test section for measuring inlet and outletwater temperatures, respectively. Fifteen thermocouples were silver soldered to the test tube surface (embedded in V-groove tube surface) for measuring local wall temperatures. The positions of the thermocouples were 15, 85, 155, 225, 295, 365, 435, 505, 575, 645, 715, 785, 855, 925 and 975 mm from the entrance of the test tube or heating section. The mean wall temperature was determined by means of calculation based on the reading of the type T thermocouples.

This material is reserved for educational use only, not allowed for commercial use.
Forbidden to modify the content, and cite the document when use.

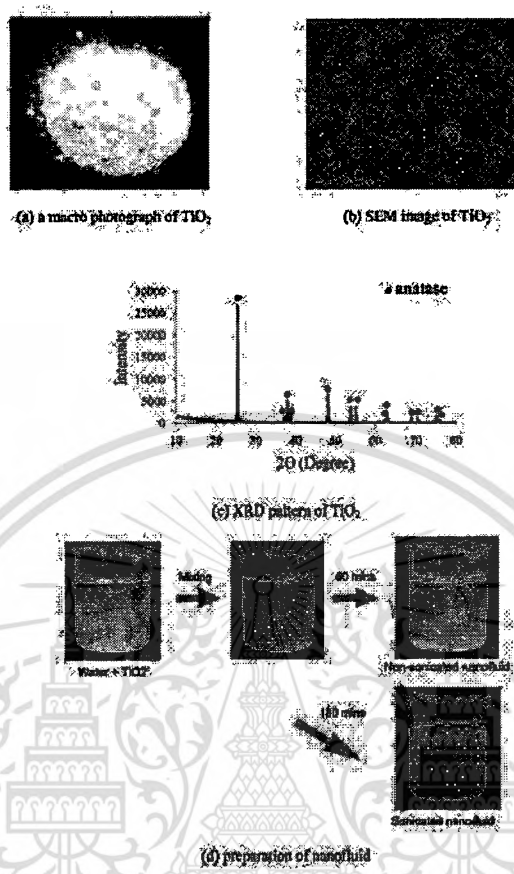

Fig. 2. Details of TiO2 nanoparticles and preparation of nanofluid using ultrasonic vibrator and SEM image of TiO2 nanoparticles: (a) a macro photograph of TiO2, (b) SEM image of TiO2, (c) XRD pattern of TiO2 and (d) preparing of nanofluid.

In the apparatus setting above, TiO2/water nanofluid was pumped to the overhead water tank then discharged through the rotameter and directed to the heat transfer test section. The data including temperature, volumetric flow rate and pressure drop is collected at steady state in which the inlet water temperature was maintained at 26 _C. The isothermal friction factor was calculated from pressure drop measured by manometer at room temperature. In the experiment, the pressure taps were located around 50 mm upstream and 100mmdownstream of the test section. The distance between both tapes was around 1150 mm. Average Nusselt number was calculated using fluid properties at the overall bulk mean temperature. Apart from dual, triple and quadruple twisted tapes, a single twisted tape was also tested for comparison. The experimental and parameter details are shown in Table 2.

This material is reserved for educational use only, not allowed for commercial use.
Forbidden to modify the content, and cite the document when use.

In the present study, the inlet Reynolds number of cold water was varied from 5400 to 15,200. Uncertainties of measurements were estimated based on ANSI/ASME [60]. The uncertainties in the axial velocity, volumetric flow rate, pressure, and temperature measurements are estimated to be within ±6%, ±4%, ±5% and ±0.5%, respectively. The accuracies of the measured quantities are 1.8 _ 10_5 kg s_1 for the mass flow rate, 0.05 _C for temperature different (DT), and 0.001 m for DL. In addition, the uncertainties of non-dimensional parameters were within ±5% for Reynolds number, ±7% for Nusselt number and ±9% for friction factor.

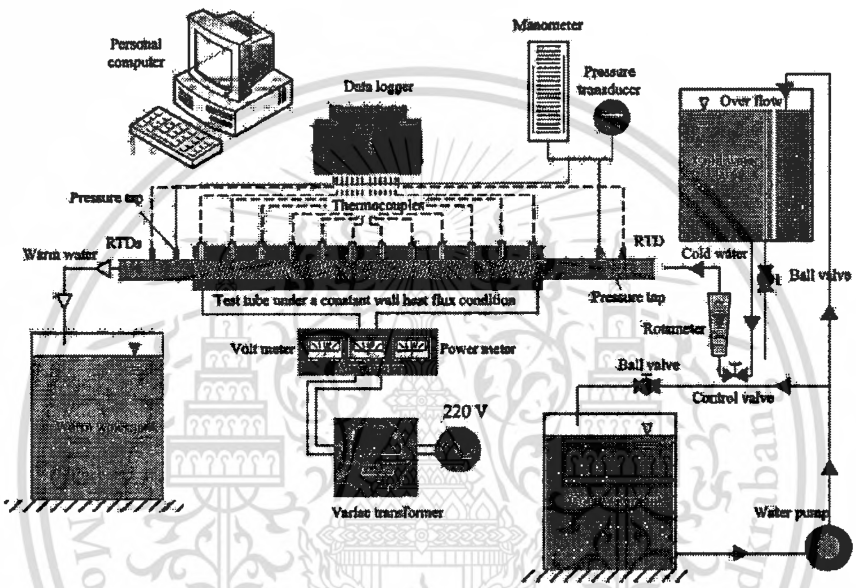

Fig. 3. Facility of experimental heat transfer set-up.

Table 2
Details of test tube and experimental conditions.

(a) Inner diameter of tube, D	19 mm
(b) Outer diameter of tube, D_o	22 mm
(c) Wall thickness of tube	1.5 mm
(d) Length of tube, L	1000 mm
(e) Material	Copper
(f) Wall condition	Constant heat flux
(g) Inlet temperature, T_i	26 °C
(h) Reynolds number, Re	5400–15,200
(i) Type of base fluid	Water
(j) Type of nanoparticle	TiO_2
(k) Average diameter of nanoparticle, d_p	15 nm
(l) Nanofluid concentrations	0.07, 0.14 and 0.21% by volume
(m) Thermal conductivity coefficient of nanoparticles, k_p	13.7 W m^{-1} K^{-1}
(n) Nanoparticle density, ρ_p	4170 kg m^{-3}
(o) Density of nanofluid, ρ_{nf}	See Eq. (9) kg m^{-3}
(p) Specific heat of nanofluid, c_{nf}	See Eq. (10) J kg^{-1} K^{-1}
(q) Thermal conductivity coefficient of nanofluid, k_{nf}	See Eq. (11) W m^{-1} K^{-1}
(r) Viscosity of nanofluid, μ_{nf}	See Eq. (12) Pa s

This material is reserved for educational use only, not allowed for commercial use.
Forbidden to modify the content, and cite the document when use.

Chapter 4

Results and Discussion

The experimental and numerical results of heat transfer enhancement by using dual, triple and quadruple twisted tapes as tube inserts and TiO2/water nanofluid as the working fluids, are reported in this section. The results of the plain tube and the tube with the single twisted tapes are also presented.

4.1. Verification of the plain tube with/without typical twisted tape

To gain confidence on experimental data throughout the research, the experimental data of the plain tube with water as the working fluid were firstly compared with those from the open literatures [66] which are DittuseBoelter and Gnielinski correlations for Nusselt number and Blasius and Petukhov correlations for the friction factor. Verification of the heat transfer and friction in the plain tube is shown in Fig. 4a. The experimental Nusselt number was in satisfactory agreement, deviated within ±3.4% and ±5.6% from the correlations of DittuseBoelter and Gnielinski, respectively while the experimental friction factors deviated within ±1.4% and ±1.8% from the correlations of Blasius and Petukhov. Fig. 4b shows the comparison between the experimental data of the present plain tube equipped with the typical/single twisted tape and those from the correlations of Manglik and Bergles [6]. Evidently, mean Nusselt number and friction factor of the tube with the typical/single twisted tape (ST) were respectively 6.1% lower and 3.8% higher than those of Manglik and Bergles equation. According to the comparative results mentioned above, it can be concluded that the present facility was reliable and experimental data was accurate enough. These provide a strong confidence in the present investigation of the heat transfer and flow friction in the tube equipped with dual/ triple/quadruple twisted tapes.

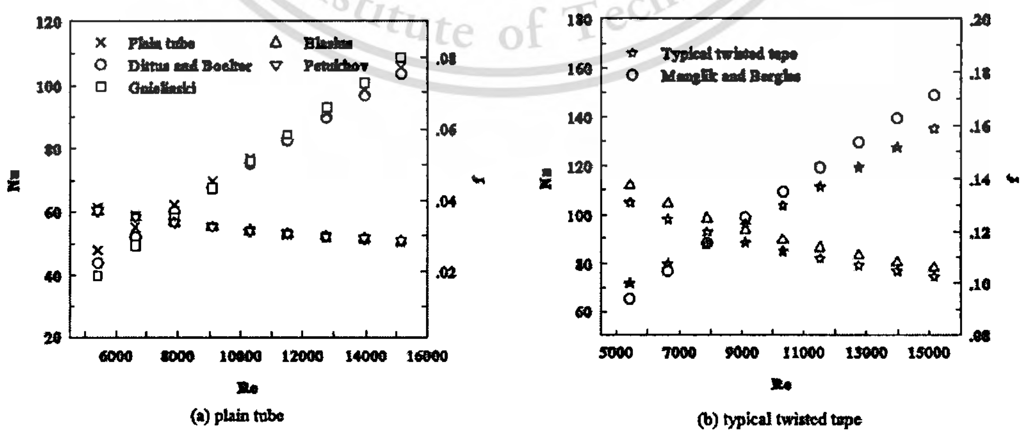

(a) plain tube

(b) typical twisted tape

Fig. 4. Validation of (a) plain tube and (b) typical twisted tape

This material is reserved for educational use only, not allowed for commercial use.
Forbidden to modify the content, and cite the document when use.

4.2. Effect of multiple twisted tapes

4.2.1. Heat transfer

The heat transfer of tubes equipped with tape insert(s) presented in terms of Nusselt number (Nut) and Nusselt number ratio (Nut/Nup), where Nup is Nusselt number for the plain tube, is shown in Fig. 5a and b. For the present work, the Reynolds number is available over the range 5400-15,200, and water was used as the working fluid. Fig. 5a shows that Nusselt number considerably increased with increasing Reynolds number. This was attributed to a stronger turbulent intensity and thus a better fluid mixing. At a given Reynolds number, Nusselt number in the tube with single/dual/triple/quadruple twisted tapes was significantly higher than those in the plain tube. This is responsible by the induction of multiple swirl flows, resulting in thinner boundary layer. Fig. 5b shows that Nusselt number ratio (Nut/ Nup) slightly decreased with increasing Reynolds number. This can be explained that at lower Reynolds number, a thermal boundary becomes thicker; therefore the swirl flows induced by twisted tapes possess more significant effect on disruption of thermal boundary. Moreover, a higher number of tape inserted in the tube consistently possessed higher Nusselt number. The tube with quadruple twisted tapes (QTs) provided the highest Nusselt number over the entire Reynolds number range. That is, Nusselt number of QTs was 16-22%, 33-45%, 100-109%, 157-215%, higher than those of the tubes with triple twisted tapes, dual twisted tapes, single twisted tape and the plain tube alone, respectively. This can be explained by the fact that more tapes induce higher number of swirl flows imparted to an axial flow, resulting in more uniform fluid mixing between the core and the tube wall regions, throughout the tube.

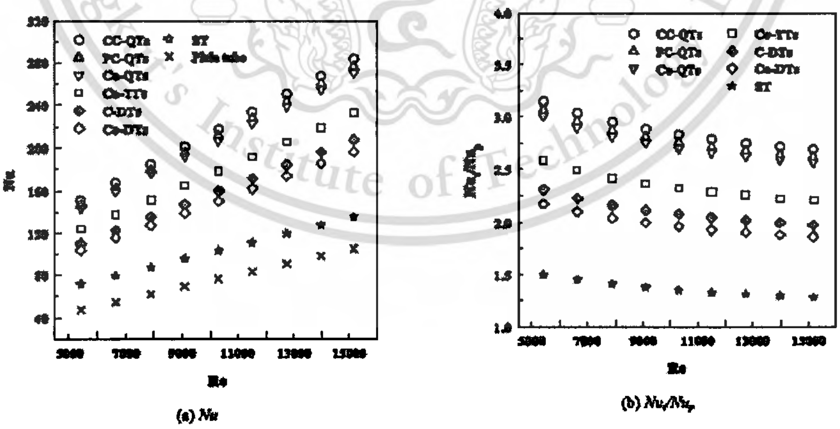

Fig. 5. Effect of dual/triple/quadruple twisted tapes on heat transfer enhancement: (a) Nu and (b) Nut/Nup.

This material is reserved for educational use only, not allowed for commercial use.
Forbidden to modify the content, and cite the document when use.

4.2.2. Friction loss

The friction loss of tubes equipped with tape inserts presented in terms of friction factor (ft) and friction factor ratio (ft/fp), where fp is friction factor for the plain tube, is shown in Fig. 6. For all the cases, friction factor slightly decreased (Fig. 6a) while friction factor ratio (ft/fp) slightly increased (Fig. 6b) with increasing Reynolds number. The effect of twisted tape on friction factor was found that friction factors generated in the tube with tape insert(s) were considerably higher than those in the plain tube. In addition, multiple-tapes inserts (dual/triple/quadruple twisted tapes) consistently caused higher friction factor than the single one. This is directly responsible by the larger surface area of the inserts which perturbed the flows within the tubes. Moreover, an increase of swirl flow number boosted the interaction of the pressure forces with inertial forces in the boundary layer. Therefore, the highest mean friction factorswere observed in quadruple twisted tapes. For co-swirl arrangement, friction factors over Co-QTs were 1.31 and 1.59 times higher than for Co-DTs (co-dual twisted tapes) and triple twisted tapes, respectively. For counter-swirl arrangement, CC-QTs generated 1.36 and 1.23 times more friction factors than C-DTs (counter-dual twisted tapes) and triple twisted tapes, respectively. The influence of multiple-tape inserts on friction factor ratio (ft/fp) was similar to that on friction factor (ft). The Co-QTs gave the highest friction factor with the maximum friction factor ratio (ft/fp) of about 11.85.

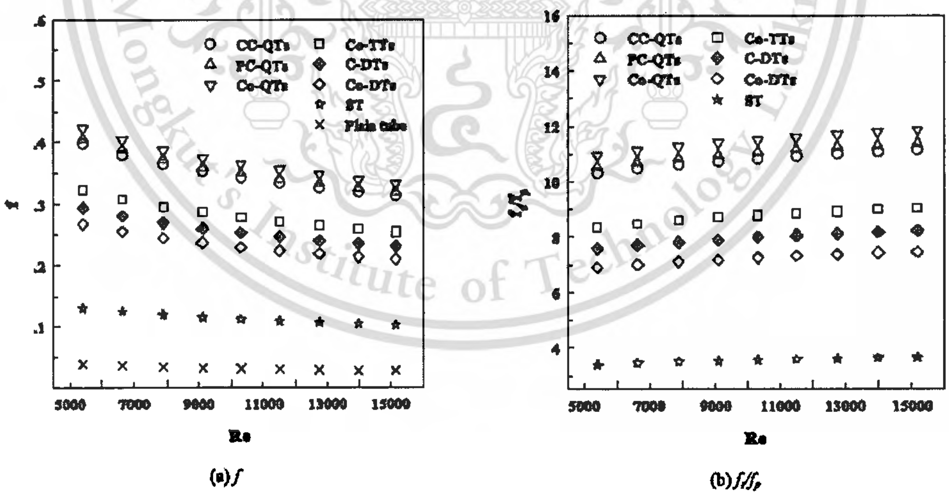

Fig. 6. Effect of dual/triple/quadruple twisted tapes on friction factor: (a) f and (b) ft/fp.

This material is reserved for educational use only, not allowed for commercial use.
Forbidden to modify the content, and cite the document when use.

สำนักหอสมุดกลาง พระจอมเกล้าลาดกระบัง

4.2.3. Thermal performance factor

Fig. 7 demonstrates the thermal performance factors (h) of tubes with tape inserts, which compromises between the heat transfer and friction loss. For a net energy gain, the value of the thermal performance factor is greater than unity. The results revealed that thermal performance factor decreased when Reynolds number increased. This implies the benefit of using tape inserts at lower Reynolds number rather than at higher Reynolds number. For a given Reynolds number, thermal performance factor increased as the number of tape inserts increased. It can be mentioned that the heat transfer enhancement by tape inserted reflects an overwhelming of increased friction loss. The thermal performance factors of the tubes with quadruple, triple and dual twisted tapes varied between 1.13 and 1.45, 1.06 and 1.27, and 0.95 and 1.18, respectively. In other words, quadruple, triple and dual twisted tapes respectively gave 35-45%, 22-27% and 14-17% higher thermal performance factors than the single tape.

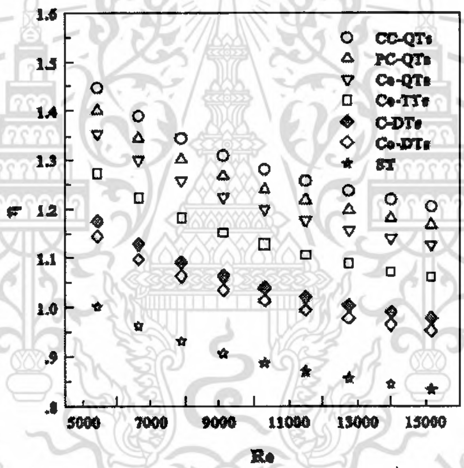

Fig. 7. Effect of dual/triple/quadruple twisted tapes on thermal performance factor.

4.3. Effect of co-/counter tape arrangement

4.3.1. Heat transfer

The effect of co-/counter tape arrangement on heat transfer enhancement can be observed from Fig. 5a and b. The tapes incounter arrangement consistently yielded higher Nusselt number than that in co-arrangement (Nu of C-DTs > Nu of Co-DTs and Nu of CC-QTs and PC-QTs > Nu of Co-QTs). Nusselt number of C-DTs was 4.8-6.5% higher than those of Co-DTs. For quadruple twisted tapes, Nusselt number of CC-QTs and PC-QTs was respectively 3.5-4.8% and 1.9-2.1% higher than those of Co-QTs. Comparing the heat transfer enhancement in counter arrangement of QTs indicated that Nusselt number of CC-QTswas 2.2-2.6% higher than that of PC-QTs.

This material is reserved for educational use only, not allowed for commercial use.
Forbidden to modify the content, and cite the document when use.
077893

4.3.2. Friction loss

The effect of co-/counter tape arrangement on friction loss is shown Fig. 6a and b. For dual twisted tapes, C-DTs consistently caused higher friction factor than Co-DTs due to a higher Nusselt number reflecting to the pressure forces, as similarly explained in Section 6.2.2. The friction factors of C-DTs were 8.2-10% higher than those of Co-DTs. However, this effect was not as pronounced for quadruple twisted tapes. Interestingly, Co-QTs possess lower Nusselt number, as seen in the previous Section of 6.2.1 (Fig. 6a), but higher friction factor than C-QTs. This is similarly observed in counter tape arrangement of QTs. A greater heat transfer of CC-QTs has a friction loss lower than PC-QTs. That is, the friction loss increased in the order CC-QTs < PC-QTs < Co-QTs. The friction factors of Co-QTs were 3.8-4.2% and 5.5-6.3% higher than those of PC-QTs and CC-QTs, respectively. In other words, friction factors of PC-QTs were 1.2e2.1% higher than those of CC-QTs.

4.3.3. Thermal performance factor

The effect of co-/counter tape arrangement on thermal performance factor at the same pumping power is shown in Fig. 7. Apparently, the tapes in counter arrangement possessed higher thermal performance factors than that in co-arrangement. Therefore, it can be mentioned that in a case of DTs the heat transfer enhancement by C-DTs reflects an overwhelming of increased friction loss. With a tubes equipped with QTs, the highest thermal performance of 1.45 was observed for CC-QTs due to their excellent heat transfer enhancement with relatively low friction loss penalty, as expected from previous Sections 6.3.1 and 6.3.2. This highlights the important role of CC-QTs in improving the performance. In addition, it can be noted that the counter tape arrangement in all cases was superior energy saving devices for the practical use, particularly at low Reynolds number. In the light of the aforementioned results, the multiple twisted tapes and co-/counter arrangements affected to heat transfer, friction loss and thermal performance factor. To clarify the reason behind the experimental results, the phenomena of swirling flow(s) in the tubes fitted with single, dual, triple and quadruple twisted tape(s) is operated via finite volume method as shown in Fig. 8a-e - 14a-e. The model conditions of are the tapes with y/ W 3.0 at constant Reynolds number of 10,000, and water was used as the working fluid. The time-averaged flow structure caused by different tapes could be discerned by considering stream function plots, which obtained via the RNG keƐ turbulence model. Each twisted tape induced a swirl flow outward from its surface. Therefore, the number of swirl flow(s) in each tubewas equal to the number of twisted tape(s). For the tube with ST in Fig. 8, turbulent kinetic energy (TKE) in the vicinity of the twisted tape surface was lower than that of other areas (Fig. 8c), especially around the upperright and lower-left of the twisted tape which corresponded to the positions of inclined to the tube

This material is reserved for educational use only, not allowed for commercial use.
Forbidden to modify the content, and cite the document when use.

wall. These parts of the tape led to the working fluid directly to the tube wall, and caused high shear stress on the wall. This promoted the heat transfer from the tube wall to the core region as reflected by the temperature field in Fig. 8d and Nusselt number distribution in Fig. 8e. For the tube with Co-DTs in Fig. 9, the turbulent kinetic energy and heat transfer by swirl flows were enhanced as compared to the tube with ST (Fig. 9b-e). In addition, the interaction between the co-dual swirl flows induced two recirculation flows as shown in tube wall, indicated by the invasion of high temperature areas around the recirculation regions (Fig. 9c). A similar phenomenon was found by C-DTs in Fig. 10. However, one recirculation zone and one impingement zone were generated instead of two recirculation zones. The presence of impingement zone resulted in high turbulent kinetic energy on the impinged wall (Fig. 10c) due to their shear force and low temperature around the impingement zone (Fig.10d). Obviously, thermal boundary layers in the tubes with DTs in co- and counter arrangements were considerably thinner than that in the tube with ST. Moreover, the areas of high Nusselt number in the tubes with Co-DTs and C-DTs (Figs. 9e and 10e) were broader than that found in the tube with ST (Fig. 8e). These evidences reveal that DTs are more efficient for the boundary disruption and thus heat transfer enhancement than ST.

King Mongkut's Institute of Technology Ladkrabang

This material is reserved for educational use only, not allowed for commercial use.
Forbidden to modify the content, and cite the document when use.

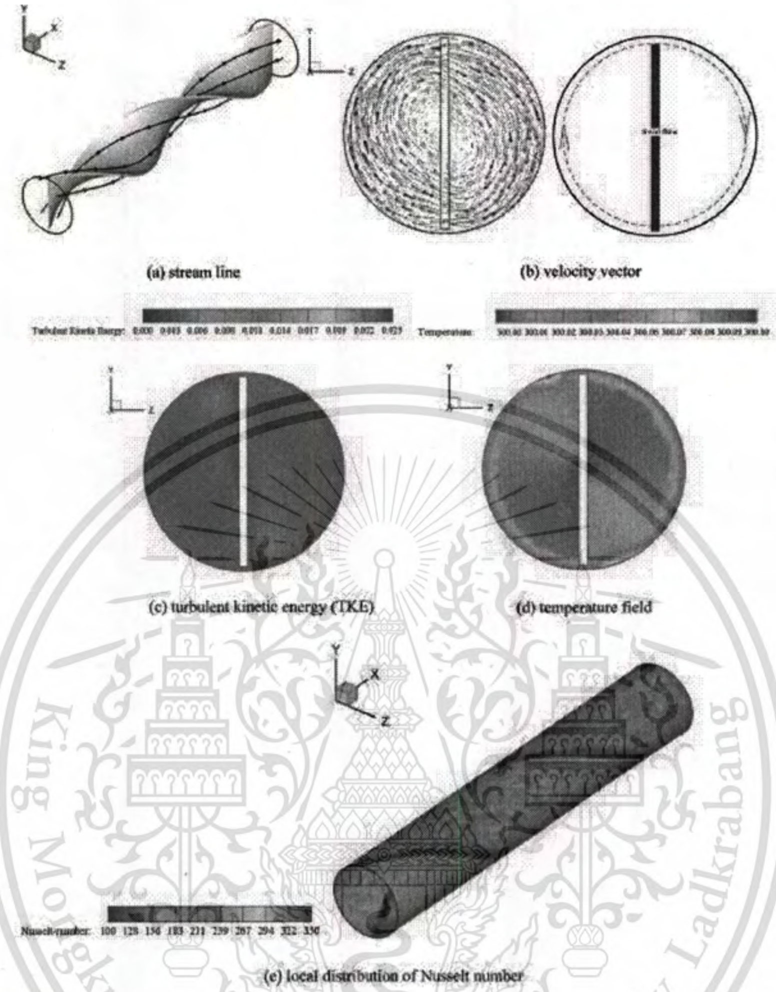

Fig. 8. Contour plots of stream line, velocity vector, turbulent kinetic energy (TKE), temperature fields and local distribution of Nusselt number in the tube fitted with ST: (a) stream line, (b) velocity vector, (c) turbulent kinetic energy (TKE), (d) temperature field and (e) local distribution of Nusselt number.

This material is reserved for educational use only, not allowed for commercial use.
Forbidden to modify the content, and cite the document when use.

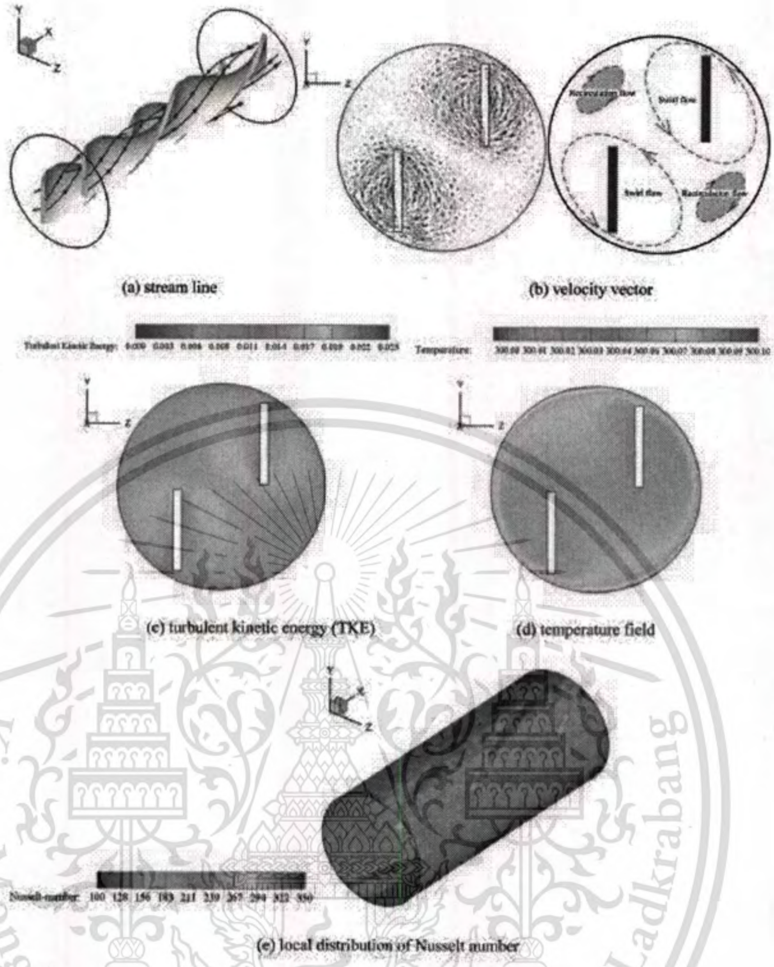

Fig. 9. Contour plots of stream line, velocity vector, turbulent kinetic energy (TKE), temperature fields and local distribution of Nusselt number in the tube fitted with Co-DTs: (a) stream line, (b) velocity vector, (c) turbulent kinetic energy (TKE), (d) temperature field and (e) local distribution of Nusselt number.

This material is reserved for educational use only, not allowed for commercial use.
Forbidden to modify the content, and cite the document when use.

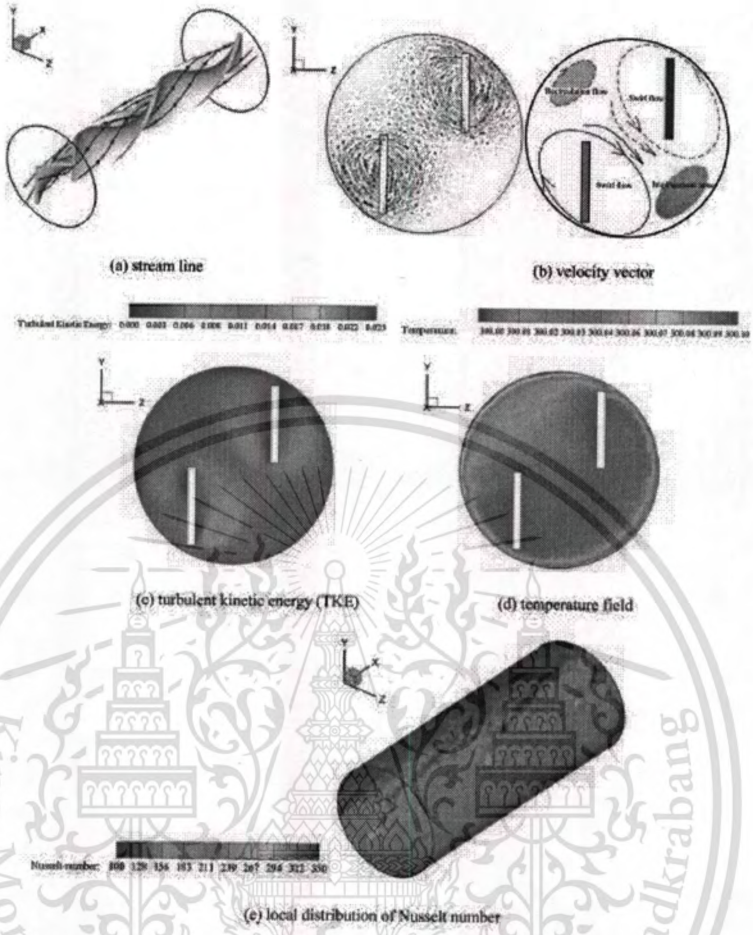

Fig. 10. Contour plots of stream line, velocity vector, turbulent kinetic energy (TKE), temperature fields and local distribution of Nusselt number in the tube fitted with C-DTs: (a) stream line, (b) velocity vector, (c) turbulent kinetic energy (TKE), (d) temperature field and (e) local distribution of Nusselt number.

This material is reserved for educational use only, not allowed for commercial use.
Forbidden to modify the content, and cite the document when use.

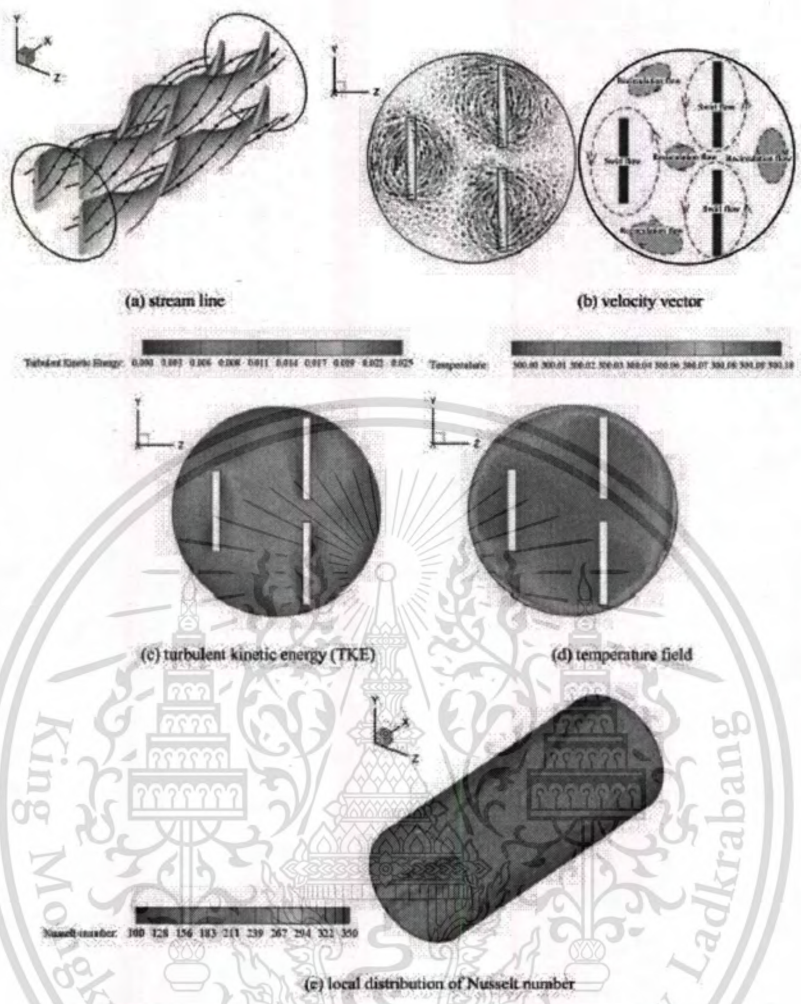

Fig. 11. Contour plots of stream line, velocity vector, turbulent kinetic energy (TKE), temperature fields and local distribution of Nusselt number in the tube fitted with Co-TTs: (a) stream line, (b) velocity vector, (c) turbulent kinetic energy (TKE), (d) temperature field and (e) local distribution of Nusselt number.

This material is reserved for educational use only, not allowed for commercial use.
Forbidden to modify the content, and cite the document when use.

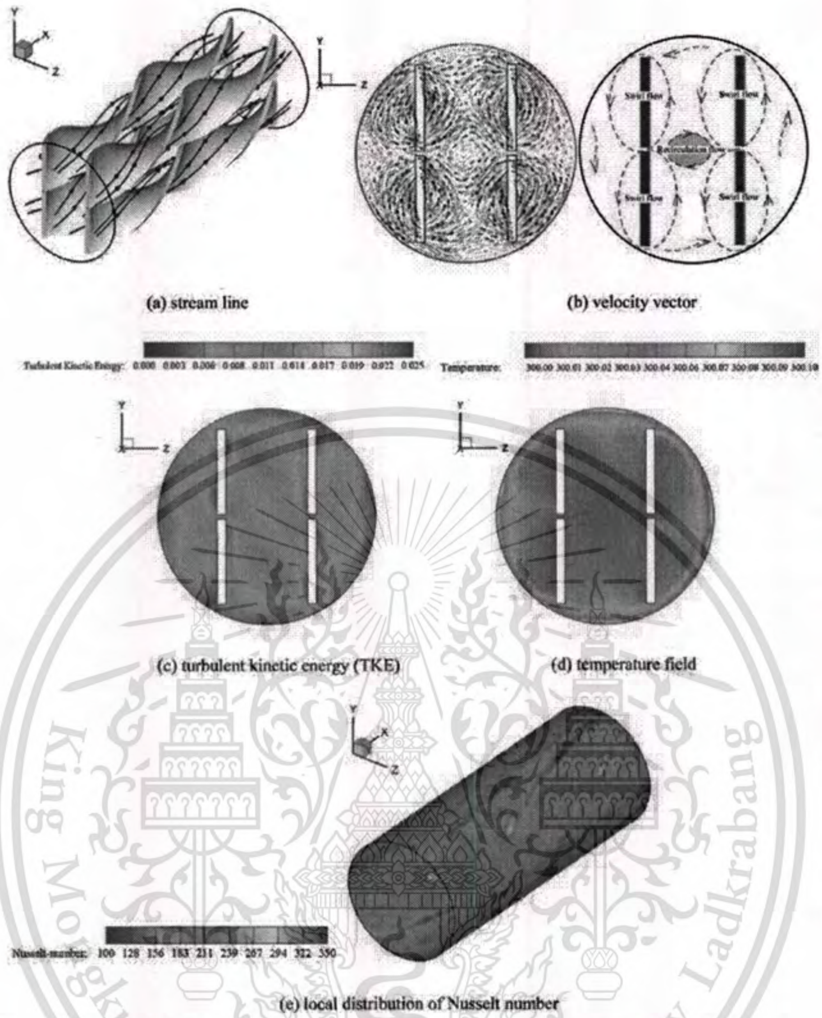

Fig. 12. Contour plots of stream line, velocity vector, turbulent kinetic energy (TKE), temperature fields and local distribution of Nusselt number in the tube fitted with Co-QTs: (a) stream line, (b) velocity vector, (c) turbulent kinetic energy (TKE), (d) temperature field and (e) local distribution of Nusselt number.

For the tube with Co-TTs in Fig. 11, three swirl flows and four recirculation zones (three zones near the tube wall and one zone in the middle of the tube were generated as shown in Fig. 11b). As compared to the tube with DT, the tube with Co-TTs showed a considerably larger area of high turbulent kinetic energy around Co-TTs (Fig. 11c), more uniform temperature field (Fig. 11d) and Nusselt distribution (Fig. 11e). These derived from better fluid mixing due to the increase of swirl number (turbulence enhancers). For the tube with Co-QTs in Fig. 12, four swirl flows and one recirculation zone in the middle of the tube were generated as shown in Fig. 12b. The tube with Co-QTs has similar phenomena to that observed for the tube with Co-TTs. However, the Co-QTs provided higher

This material is reserved for educational use only, not allowed for commercial use.
Forbidden to modify the content, and cite the document when use.

turbulent intensity kinetic energy, more uniform temperature filed and Nusselt number distribution, as compared to Co-TTs. For the tube with PC-QTs in Fig.13, the upper pair of twisted tapes produced two swirl flows in the same direction which was opposite to that of the lower pair. Only one small impingement zone was inducing without recirculation zone as shown in Fig. 13b. The interaction between the swirl flows induced by the upper, and lower tapes induced impingement zone on the right wall. This resulted in high turbulent intensity kinetic energy (Fig. 13c) and thin thermal boundary layer around the right wall of the tube (Fig.13d). The high momentum of fluid on the wall directly promotes heat transfer from the impinged surface. Comparatively, PC-QTs provided considerably more uniform Nusselt number distribution than Co-QTs. For the tube with CC-QTs in Fig. 14, four swirl flows were simultaneously directed to the tube core. The interaction between swirl flows produced from the tapes in the left pair induced a small impingement zone on the left wall. Similarly, the tapes in the right pair induced another impingement zone on the rightwall. The interaction among the swirl flows resulted in five zones with high turbulent kinetic energies (four zones near tube wall and one zone in the middle of the tube), covering almost the cross section area, and reflected to a chaotic fluid mixing within the tube. The above phenomena led to excellent heat transfer indicated by thin thermal boundary layer (Fig. 14d) and high Nusselt number (Fig. 14e) almost on the whole surface of the tube. Regarding to results in Figs.12e,13e and 14e, the tube with CC-QTs possessed slightly higher Nusselt number than the tube with PC-QTs while the uniformities of Nusselt number distributions in both tubes were comparable. However, both CC-QTs and PC-QTs offered more uniform Nusselt number distributions with higher value of Nusselt number than Co-QTs. It can be concluded that the increase of twisted tape number offered better heat transfer due to more consistent swirl flows within the tube. Moreover, the interaction among the tapes also induced recirculation flows and impinging streams which provided an extra fluid mixing and additional heat transferenhancement between tube wall and core region. The impinging streams were more efficient for heat transfer enhancement by recirculation flows.

This material is reserved for educational use only, not allowed for commercial use.
Forbidden to modify the content, and cite the document when use.

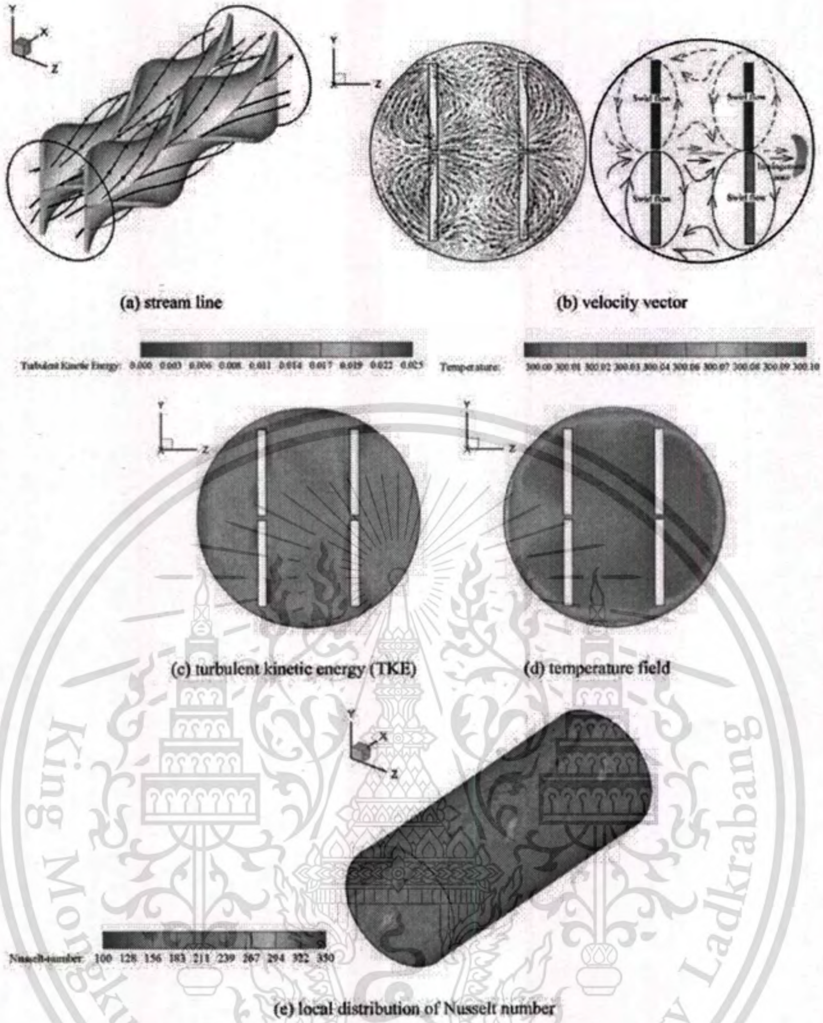

Fig. 13. Contour plots of stream line, velocity vector, turbulent kinetic energy (TKE), temperature fields and local distribution of Nusselt number in the tube fitted with PC-QTs: (a) stream line, (b) velocity vector, (c) turbulent kinetic energy (TKE), (d) temperature field and (e) local distribution of Nusselt number.

This material is reserved for educational use only, not allowed for commercial use.
Forbidden to modify the content, and cite the document when use.

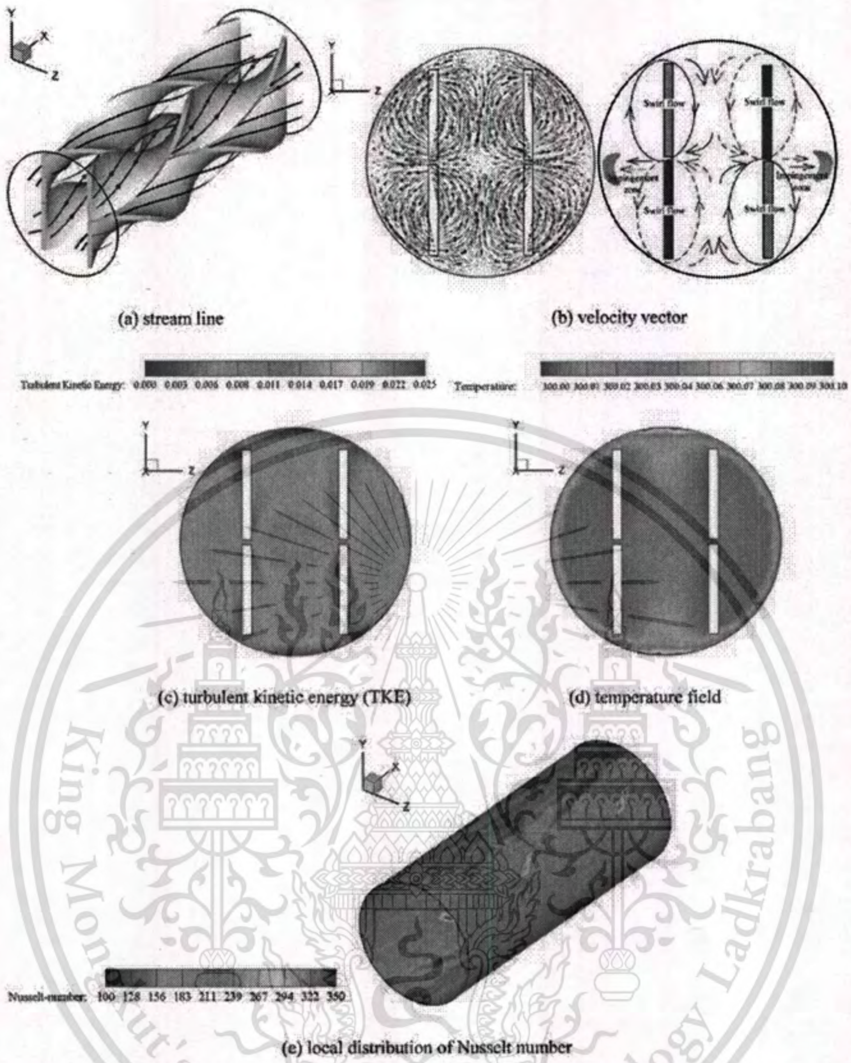

Fig. 14. Contour plots of stream line, velocity vector, turbulent kinetic energy (TKE), temperature fields and local distribution of Nusselt number in the tube fitted with CC-QTs: (a) stream line, (b) velocity vector, (c) turbulent kinetic energy (TKE), (d) temperature field and (e) local distribution of Nusselt number.

This material is reserved for educational use only, not allowed for commercial use.
Forbidden to modify the content, and cite the document when use.

4.4. Effect of nanofluid concentration

4.4.1. Heat transfer

Fig. 15a and b presents heat transfer results of the TiO2/water nanofluids (0.07%, 0.14% and 0.21% by volume) in accompanies with multiple twisted tapes. It was found that heat transfer (Nusselt number) increased when increasing nanofluid concentration. For the tubes with twisted tapes, the average Nusselt number of nanofluid with TiO2 concentrations of 0.07%, 0.14% and 0.21% by volume, was around 3.6e6.2%, 5.2e8.8% and 7.5e11.8% those of the base fluid (water). In other words, nanofluid with TiO2 concentration of 0.21% by volume gave 4.5% and 2.8% higher Nusselt number than the ones with TiO2 concentrations of 0.07% and 0.14% by volume, respectively. Moreover, the increase of nanoparticle loading also offers higher contact area between nanoparticles and the base fluid as well as twisted tapes. The enhanced heat transfer is due to thermal conductivity and collision of nanoparticles. In particular, using CC-QTs induced an effective swirl flows in enhancing nanofluid exchange between the core and the wall regions and thus increasing convective heat transfer. As nanofluid with TiO2 concentration was used, Nusselt number of CC-QTs was 3.1e3.7% and 4.8e6.3% higher than that of PC-QTs and Co-QTs, respectively. However, loading too much nanoparticles into nanofluid beyond the optimum concentration may diminish the fluid movement and heat transfer rate due to increased fluid viscosity. In the present work, the decrease of Nusselt number was not found when increasing in concentration. This implies the present nanofluid concentration range did not exceed the optimum level. Therefore, the effect of TiO2 nanoparticles was more pronounced for thermal conductivity and the collision than viscosity.

4.4.2. Friction loss

The effect of nanofluid concentration on friction factor is shownin Fig. 16a and b. For the present range, nanofluid with TiO2 concentrations of 0.07%, 0.14% and 0.21% by volume respectively caused 1.9%, 3.8% and 5.3% higher friction factor compared to those of the base fluid. In other words, nanofluid with TiO2 concentration of 0.21% by volume caused 3.3% and 1.5% higher friction factors than the ones with TiO2 concentrations of 0.07% and 0.14% by volume, respectively. As nanofluid with TiO2 concentration was used, the friction factors of Co-QTs were 2.4-4.2% and 3.2-6.3% higher than those of PC-QTs and CC-QTs, respectively. The increase of friction loss is directly caused by the increases of fluid viscosity and shear force on tube wall acted by nanoparticles. In particular, at low Reynolds number all nanofluid yielded higher pressure loss than the base fluid. However, the results indicate that utilizing nanofluid in the present concentration range is an insignificant friction loss penalty.

This material is reserved for educational use only, not allowed for commercial use.
Forbidden to modify the content, and cite the document when use.

4.4.3. Thermal performance factor

Fig. 17 shows the effect of nanofluid concentration on thermal performance factor. Evidently, nanofluid with higher TiO2 concentrations yielded higher thermal performance factors. Depending on Reynolds number, thermal performance factors given by nanofluid with TiO2 concentrations of 0.07%, 0.14% and 0.21% by volume were 0.86-1.53, 0.87-1.55 and 0.88-1.59, respectively. Comparatively, nanofluid with TiO2 concentration of 0.21% by volume offered 3.4% and 2.3% higher thermal performance factors than the ones with TiO2 concentrations of 0.07% and 0.14% by volume, respectively. This indicates the effect of increasing TiO2 nanoparticles on thermal performance factor was more pronounced for the heat transfer improvement as positive effect than friction loss as negative effect in a range of Reynolds number 5400-15,200, especially at lower Reynolds number where pressure losses were insignificant. As nanofluid with TiO2 concentration was used, the thermal performance of Co-QTs, PC-QTs and CC-QTs was 1.17-1.47, 1.22-1.53 and 1.27-1.59, respectively.

King Mongkut's Institute of Technology Ladkrabang

This material is reserved for educational use only, not allowed for commercial use.
Forbidden to modify the content, and cite the document when use.

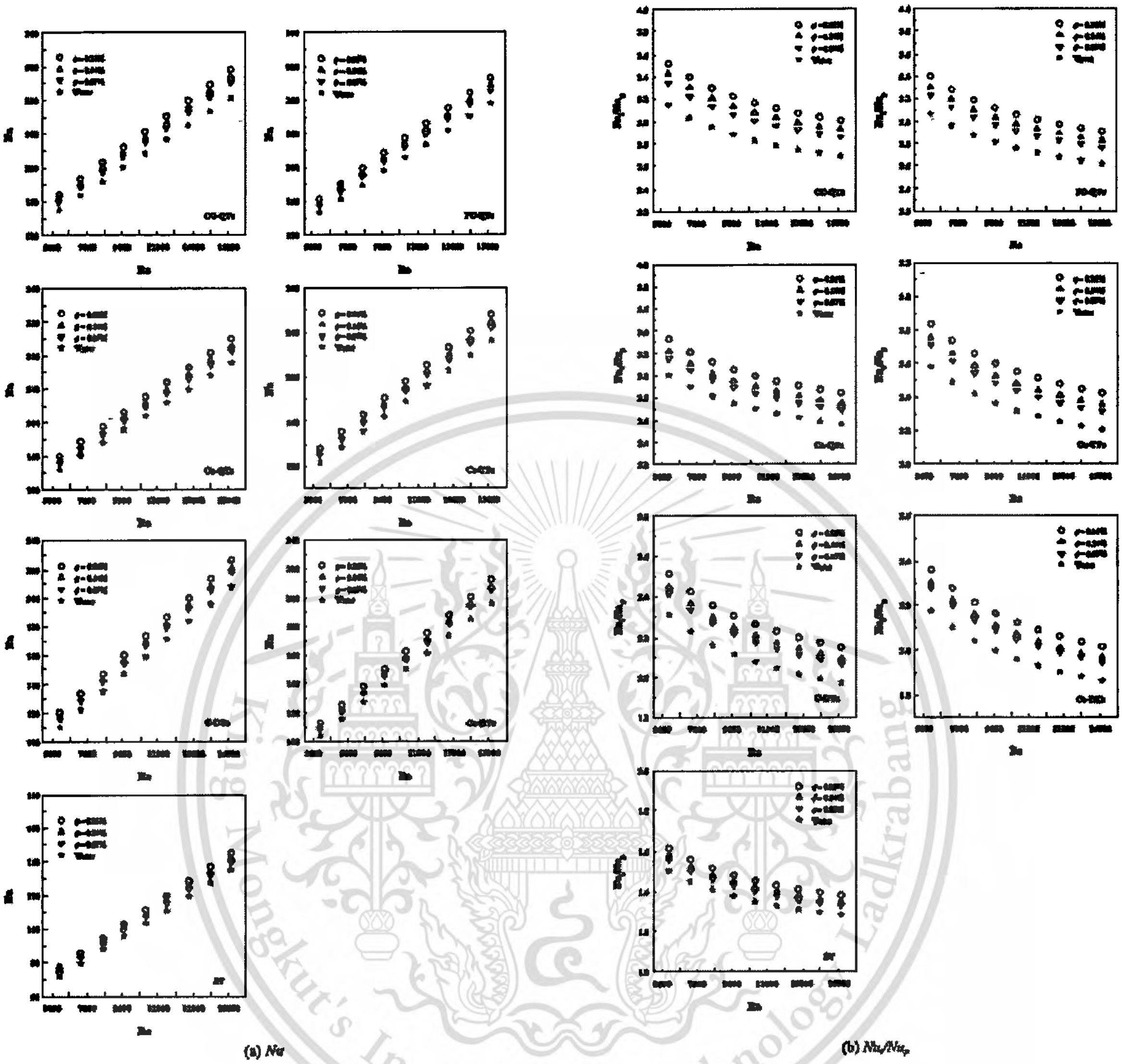

Fig. 15. Effect of TiO2 concentration on heat transfer enhancement: (a) Nu and (b) Nut/Nup.

This material is reserved for educational use only, not allowed for commercial use.
Forbidden to modify the content, and cite the document when use.

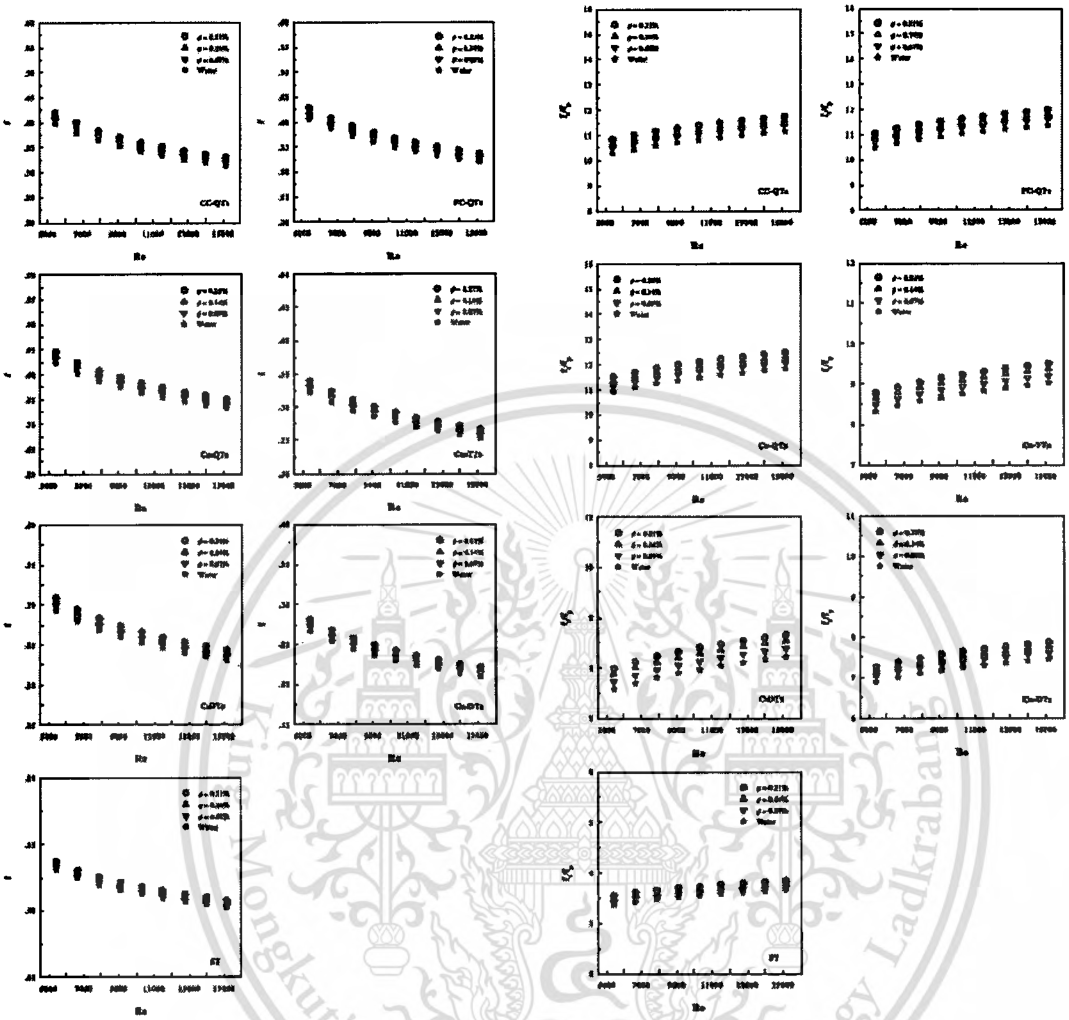

Fig. 16. Effect of TiO2 concentration on friction factor: (a) f and (b) ft/fp.

This material is reserved for educational use only, not allowed for commercial use.
Forbidden to modify the content, and cite the document when use.

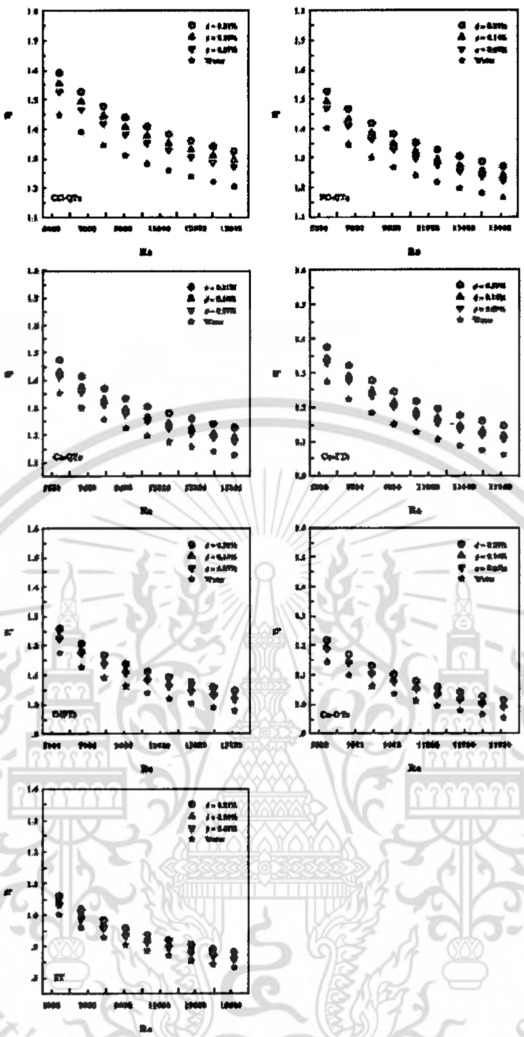

Fig. 17. Effect of TiO2 concentration on thermal performance factor.

4.5. Empirical correlations

Experimental results were applied to develop the correlations for Nusselt number, friction factor and thermal performance factor of tubes with dual/triple/quadruple twisted tapes in co-/counter tape arrangement when TiO2/water nanofluid was used as working fluids. The correlations were developed by curve fitting of experimental data. Resultant correlation is obtained in terms of Reynolds number (Re), number of tapes (N), and the TiO2 concentrations (f) as shown in Eqs. (32) through (40).

For tube fitted with single tape (ST), dual co tapes (Co-DTs) triple co tapes (Co-TTs) and quadruple co tapes *(Co-QTs):*

This material is reserved for educational use only, not allowed for commercial use.
Forbidden to modify the content, and cite the document when use.

$$Nu = 0.103\,\mathrm{Re}^{0.618}\,\mathrm{Pr}^{0.4}(1+N)^{0.768}\left(1+\phi\right)^{0.438} \tag{24}$$

$$f = 0.429\,\mathrm{Re}^{-0.234}(1+N)^{1.276}\left(1+\phi\right)^{0.899} \tag{25}$$

$$\eta = 3.618\,\mathrm{Re}^{-0.178}(1+N)^{0.343}\left(1+\phi\right)^{0.138} \tag{26}$$

For tube fitted with single tape (ST), dual counter tapes (C-DTs), quadruple counter tapes in parallel counter-swirl flow arrangement (PC-QTs):

$$Nu = 0.104\,\mathrm{Re}^{0.618}\,\mathrm{Pr}^{0.4}(1+N)^{0.789}\left(1+\phi\right)^{0.439} \tag{27}$$

$$f = 0.457\,\mathrm{Re}^{-0.233}(1+N)^{1.248}\left(1+\phi\right)^{0.926} \tag{28}$$

$$\eta = 3.558\,\mathrm{Re}^{-0.178}(1+N)^{0.374}\left(1+\phi\right)^{0.129} \tag{29}$$

For tube fitted with quadruple counter tapes in cross counter-swirl flow arrangement (CC-QTs):

$$Nu = 0.096\,\mathrm{Re}^{0.618}\,\mathrm{Pr}^{0.4}(1+N)^{0.834}\left(1+\phi\right)^{0.468} \tag{30}$$

$$f = 0.401\,\mathrm{Re}^{-0.233}(1+N)^{1.271}\left(1+\phi\right)^{0.953} \tag{31}$$

$$\eta = 3.444\,\mathrm{Re}^{-0.178}(1+N)^{0.411}\left(1+\phi\right)^{0.149} \tag{32}$$

Figure 18(a-c) shows comparison between experimental data and predicted data which were calculated from the correlations. Apparently, predicted data were in good agreements with experimental data with deviations within ±5.4% to ±10.3%, ±6.6% to ±19% and ±1.5% to ±3% for Nusselt number, friction factor and thermal performance factor, respectively. Note that above empirical correlations are suitable for the systems with TiO_2/water nanfluids when TiO_2 concentrations $\leq$0.21% by volume and Reynolds number between 5400 and 15,200.

This material is reserved for educational use only, not allowed for commercial use.
Forbidden to modify the content, and cite the document when use.

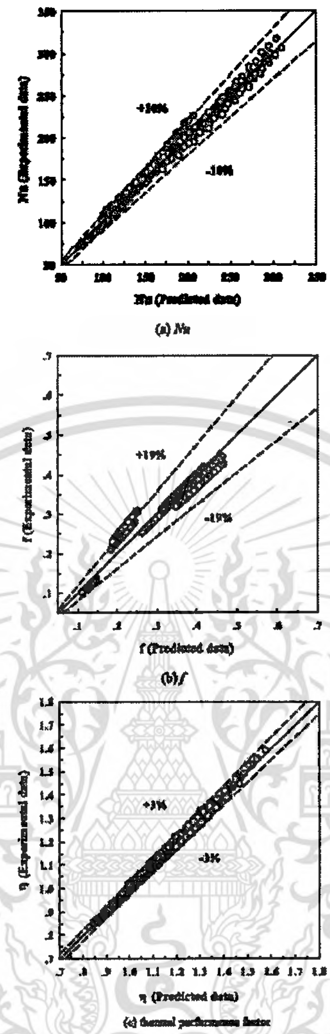

Fig. 18. Comparisons between predicted data via the empirical correlations and experimental data: (a) Nusselt number, (b) friction factor and (c) thermal performance factor.

This material is reserved for educational use only, not allowed for commercial use.
Forbidden to modify the content, and cite the document when use.

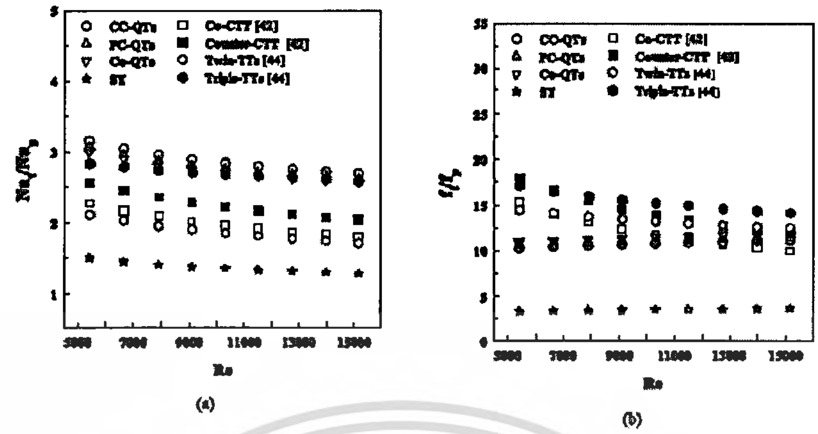

Fig. 19. Comparisons between the results of the present modified twisted tapes and those of the previous modified twisted tapes: (a) Nut/Nup & Re and (b) ft/fp & Re.

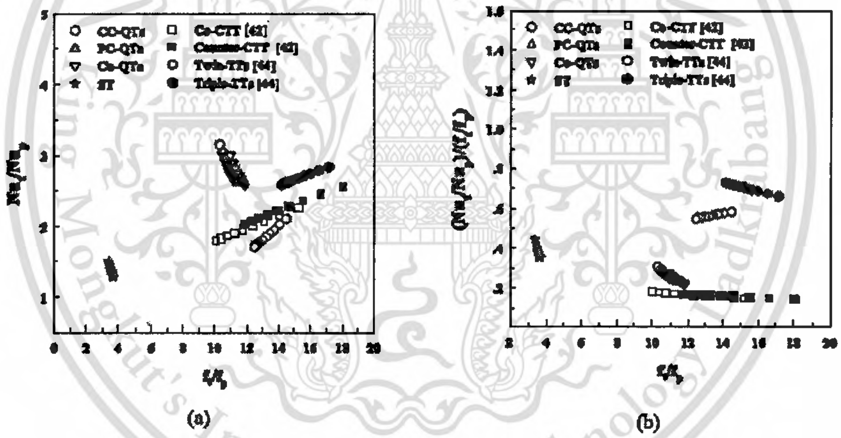

Fig. 20. Comparisons between the results of the present modified twisted tapes and those of the previous modified twisted tapes: (a) Nut/Nup & ft/fp and (b) (Nut/Nup)/(ft/ fp) & ft/fp.

This material is reserved for educational use only, not allowed for commercial use.
Forbidden to modify the content, and cite the document when use.

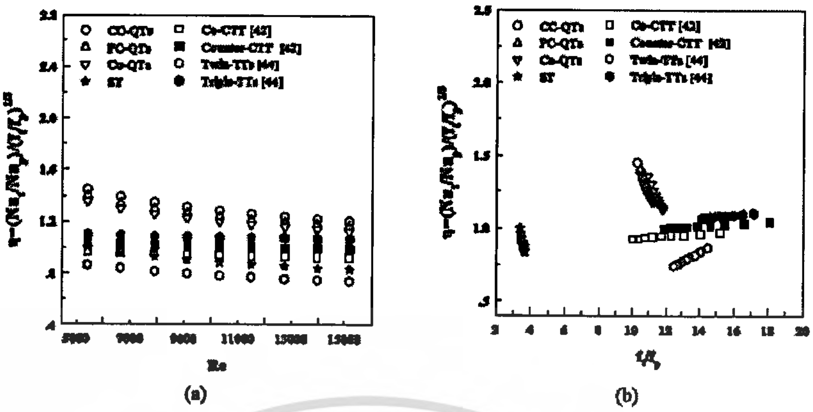

Fig. 21. Comparisons between the results of the present modified twisted tapes and those of the previous modified twisted tapes: (a) (Nut/Nup)/(ft/fp)1/3 & Re and (b) (Nut/ Nup)/(ft/fp)1/3 & ft/fp.

4.6. Overall comparisons

As shown in Fig. 19a and b, the uses of the present modified multiple twisted tapes (Co-QTs, CC-QTs and PC-QTs) and the previous modified multiple twisted tapes including coupling twisted tapes in co-arrangement (co-CTT) [42], coupling twisted tapes in counter arrangement (counter-CTT) [42], twin twisted tape (Twin- TTs) [44] and triple twisted tapes (Triple-TTs) [44] resulted in considerably higher Nusselt number and friction than those found by the uses of single/typical twisted tape (ST). This is attributed to the higher turbulence intensities and more chaotic fluid mixing caused by the interaction of swirl flows induced by the multiple tapes. Evidently, Nusselt number and friction factor values of the modified twisted tape are higher than those of the ST in a range of 1.45e2.1 times and 2.04e3.05 times of ST, respectively. In addition, Nusselt numbers of the present quadruple twisted tapes (Co-QTs,nCC-QTs and PC-QTs) are higher than those of the multiple twisted tapes in the previous works which are counter-CTT [42], co-CTT [42], twin-TTs [44], and triple-TTs [44], around 185e216%, 223e258%, 57e78% and 8e25%, respectively. On the other hand, the friction factors caused by quadruple twisted tapes are lower than those caused by the previously modified tapes at low Reynolds number, but they become comparable at high Reynolds number. To examine the variations over this friction factor ratio range, the heat transfer augmentation (Nut/Nup) and the ratio between heat transfer augmentation and friction factor augmentation (ft/fp) are plotted against ft/fp from 2 to 18 in Fig. 20a. It is found that the present quadruple twisted tapes (Co-QTs, CC-QTs and PC-QTs) offered higher heat transfer augmentation accompanying with lower friction factor enhancement as compared to those given by the tape inserts in the previous works [42,44]. It is also observed that

This material is reserved for educational use only, not allowed for commercial use.
Forbidden to modify the content, and cite the document when use.

heat transfer augmentation (Nut/Nup) and friction factor augmentation (ft/fp) given by ST are lower than those given by all examined multiple tapes. The maximum ft/fp given by ST is 3.7 while that given by counter-CTT is as high as 18 [42]. The (Nut/Nup)/ (ft/fp) parameter, presented in Fig. 20b, is referred as the Reynolds analogy performance parameter. Among the examined tapes, the triple-TTs give the highest (Nut/Nup)/(ft/fp) while co-CTTs [42] and counter-CTTs [42] give the lowest (comparable) one. The (Nut/Nup)/ (ft/fp) given by the present quadruple twisted tapes (QTs) lie between those of triple-TTs and CTTs. All of multiple-tapes insert gives higher heat transfer augmentations and higher increases in pressure losses than ST. The thermal performance factors ((Nut/Nup)/(ft/fp)1/3) in tubes equipped with the present quadruple twisted tapes (QTs) and other multiple twisted tapes inserts in the previous works counter-CTT [42], co-CTT [42], twin-TTs [44], and triple-TTs [44] are demonstrated in Fig. 21a. The thermal performance factors are evaluated at a constant pumping power. For all cases, thermal performance factors decrease with increasing Reynolds number. Comparatively, thermal performance factors given by present CC-QTs are slightly higher than those offered by counter-CTT [42], co-CTT [42], twin-TTs [44], and triple-TTs [44] around 13e39%, 22e50%, 52e68% and 5e31%, respectively. In general, the thermal performance factors ((Nut/Nup)/(ft/fp)1/3) of the modified twisted tapes are higher than those of the ST around 1.14e1.45 depending on the twisted tape types. Fig. 20b shows variation between ((Nut/Nup)/(ft/fp)1/3) and friction factor ratio (ft/fp). As presented, the present quadruple twisted tapes (Co-QTs, CC-QTs and PC-QTs) give higher thermal performance than other tapes at the same friction factor ratio.

This material is reserved for educational use only, not allowed for commercial use.
Forbidden to modify the content, and cite the document when use.

Chapter 5

Conclusions

The influences of multiple twisted tapes with a co- or counter- arrangements (e.g., *ST, Co-DTs, Co-TTs, Co-QTs, C-DTs, PC-QTs, CC-QTs*) and TiO_2 nanoparticles in water as a working fluid on heat transfer enhancement are described in this study. The experimental results are compared with the tube equipped with plain tube and typical twisted tape inserts. The conclusions are drawn below:

- Nusselt number, friction factor and thermal performance factor increased as a number of tapes increased.
- The tapes in counter arrangement provided higher thermal performance factor than that in co-arrangement, Interestingly, *CC-QTs* exhibited superior twisted ape which delivers not only high Nusselt number but also low friction factor.
- The benefit of TiO_2 nanoparticles in water was significant in improving thermal performance. TiO_2 nanoparticles exhibited a continual increase in thermal performance with increasing concentration.
- Over the range of Reynolds number 5400-15,200, Nusselts number in tubes with the *C-DTs, Co-DTs, Co-TTs, Co-QTs, PC-QTs* and *CC-QTs* was, respectively, 97.4-151.4%, 86.2-135.8%, 120.9-183.9%, 156.8-232.9%, 162.2-240%, and 169-251.9%, higher than that of the plain tube. The enhanced Nusselt number was accompanied with friction factors around 7.58-9.84, 6.89-8.81, 8.34-11.0, 10.94-14.67, 10.5-14.19, and 10.29-14.02 times over that of the plain tube.
- Thermal performance factors for *Co-DTs, Co-TTs, Co-QTs, C-DTs, PC-QTs* and *CC-QTs,* were found to be 0.95-1.17, 1.06-1.31, 1.12-1.40, 0.98-1.2, 1.17-1.44, and 1.2-1.5, respectively.
- The thermal performance factors of the nanofluid with TiO_2 concentrations of 0.07%, 0.14% and 0.21% by volume were respectively 0.5-1.7%, 1.5-2.7% and 2.1-3.6% higher than that of the based fluid (water).
- The empirical correlations developed for Nusselt number, friction factor and thermal performance factor agree well with the experimental data.

This material is reserved for educational use only, not allowed for commercial use.
Forbidden to modify the content, and cite the document when use.

Chapter 6

Benefits

This research work has proposed the potential solutions of heat transfer enhancement in heat exchangers. Nanofluid was utilized together with other heat transfer enhancement devices, especially twisted tapes is well attractive way for heat transfer enhancement with insignificant friction loss. The benefits are as follows;

1. Obtain the suitable concentration of nanoparticles with twisted tapes which enhance heat transfer enhancement in heat exchangers
2. Obtain new knowledge and publish such knowledge in international journal recognized in ISI Web of Science. The title and journal publication is "Heat transfer enhancement by multiple twisted tape inserts and TiO2/water nanofluid" in Applied Thermal Engineering, impact factor 2.624

King Mongkut's Institute of Technology Ladkrabang

This material is reserved for educational use only, not allowed for commercial use.
Forbidden to modify the content, and cite the document when use.

References

[1] J.M. Whitham, The effects of retarders in fire tubes of steam boilers, Street Railway Journal 12 (1896) 374.

[2] R.L. Webb, Performance evaluation criteria for use of enhanced heat transfer surfaces in heat exchanger design, International Journal of Heat and Mass Transfer 24 (1981) 715-726.

[3] G.C. Kidd Jr., Heat transfer and pressure drop for nitrogen flowing in tubes containing twisted tapes, AIChE Journal 15 (1969) 581-585.

[4] L. Wang, B. Sunden, Performance comparison of some tube inserts, International Communication in Heat and Mass Transfer 29 (2002) 45-56.

[5] O.H. Klepper, Heat transfer performance of short twisted tapes, AIChE Joutnal 35 (1972) 1-24.

[6] R.M. Manglik and A.E. Bergles, Heat transfer and pressure drop correlations for twisted-tape inserts in isothermal tubes: Part II-Transition and turbulent flows, Transaction of ASME, Journal Heat Transfer 115 (1993) 890-896.

[7] A.W. Date, U.N. Gaitonde, Development of correlations for predicting characteristics of laminar flow in a tube fitted with regularly spaced twisted-tape elements, Experimental Thermal Fluid Science 3 (1990) 373-382.

[8] S. Eiamsa-ard, C. Thianpong, P. Promvonge, Experimental investigation of heat transfer and flow friction in a circular tube fitted with regularly spaced twisted elements, International Communications in Heat and Mass Transfer 33 (2006) 1225-1233.

[9] A. Dewan, P. Mahanta, K. Sumithra Raju, P. Suresh Kumar, Review of passive heat transfer augmentation techniques, Journal of Power Energy 218 (2004) 509-525.

[10] S. Eiamsa-ard, P. Seemawute, K. Wongcharee, Influences of peripherally-cut twisted tape insert on heat transfer and thermal performance characteristics in laminar and turbulent tube flows, Experimental Thermal and Fluid Science 34 (2010) 711-719.

[11] S. Eiamsa-ard, K. Wongcharee, P. Eiamsa-ard, C. Thianpong, Heat transfer enhancement in a tube using delta-winglet twisted tape inserts, Applied Thermal Engineering 30 (2010) 310-318.

[12] S. Eiamsa-ard, K. Wongcharee, P. Eiamsa-ard, C. Thianpong, Thermohydraulic investigation of turbulent flow through a round tube equipped with twisted tapes consisting of centre wings and alternate-axes, Experimental Thermal and Fluid Science 34 (2010) 1151-1161.

This material is reserved for educational use only, not allowed for commercial use.
Forbidden to modify the content, and cite the document when use.

[13] Y. Wang, M. Hou, X. Deng, L. Li, C. Huang, H. Huang, G. Zhang, Ch. Chen, W. Huang, Configuration optimization of regularly spaced short-length twisted tape in a circular tube to enhance turbulent heat transfer using CFD modeling, Applied Thermal Engineering 31 (2011) 1141-1149.

[14] S. Eiamsa-ard, K. Wongcharee, S. Sripattanapipat, 3-D numerical simulation of swirling flow and convective heat transfer in a circular tube induced by means of loose-fit twisted tapes, International Communications in Heat and Mass Transfer, 36 (2009) 947-955.

[15] S. Eiamsa-ard, P. Promvonge, Thermal characteristics in round tube fitted with serrated twisted tape, Applied Thermal Engineering 30 (2010) 1673-1682.

[16] J. Guo, A. Fan, X. Zhang, W. Liu, A numerical study on heat transfer and friction factor characteristics of laminar flow in a circular tube fitted with center-cleared twisted tape, International Journal of Thermal Sciences 50 (2011) 1263-1270.

[17] C. Yong-Zhang, T. Mao-Cheng, Three-dimensional numerical simulation of thermalhydraulic performance of a circular tube with edgefold-twisted-tape inserts, Journal of Hydrodynamics 22 (2010) 662-670.

[18] S. Eiamsa-ard, K. Wongcharee, P. Promvonge, Influence of non-uniform twisted tape on heat transfer enhancement characteristics, Chemical Engineering Communication 199 (2012) 1279-1297.

[19] P. Seemawute, S. Eiamsa-ard, Thermohydraulics of turbulent flow through a round tube by a peripherally-cut twisted tape with an alternate axis, International Communications in Heat and Mass Transfer 37 (2010) 652-659.

[20] S. Eiamsa-ard, P. Promvonge, Performance assessment in a heat exchanger tube with alternate clockwise and counter-clockwise twisted-tape inserts, International Journal of Heat and Mass Transfer 53 (2010) 1364-1372.

[21] K. Wongcharee, S. Eiamsa-ard, Friction and heat transfer characteristics of laminar swirl flow through a round tube inserted with alternate clockwise and counter-clockwise twisted-tapes, International Communications in Heat and Mass Transfer 38 (2011) 348-352.

[22] P. Bharadwaj, A.D. Khondge, A.W. Date, Heat transfer and pressure drop in a spirally grooved tube with twisted tape insert, International Journal of Heat and Mass Transfer 52 (7-8) (2009) 1938-1944.

[23] S.K. Saha, U.N. Gaitonde, A.W. Date, Heat transfer and pressure drop characteristics of laminar flow in a circular tube fitted with regularly spaced twisted-tape elements, Experimental Thermal Fluid Science 2 (1989) 310-322.

[24] C. Thianpong, P. Eiamsa-ard, S. Eiamsa-ard, Heat transfer and thermal performance characteristics of heat exchanger tube fitted with perforated twisted-tapes, Heat Mass Transfer 48 (2012) 881-892.

This material is reserved for educational use only, not allowed for commercial use.
Forbidden to modify the content, and cite the document when use.

[25] M. Rahimi, S.R. Shabanian, A.A. Alsairafi, Experimental and CFD studies on heat transfer and friction factor characteristics of a tube equipped with modified twisted tape inserts, Chemical Engineering and Processing: Process Intensification 48 (2009) 762-770.

[26] P. Sivashanmugam, S. Suresh, Experimental studies on heat transfer and friction factor characteristics of laminar flow through a circular tube fitted with helical screw-tape inserts, Applied Thermal Engineering 26 (2006) 1990-1997.

[27] P. Sivashanmugam, S. Suresh, Experimental studies on heat transfer and friction factor characteristics of turbulent flow through a circular tube fitted with helical screw-tape inserts, Chemical Engineering and Processing: Process Intensification 46 (2007) 1292-1298.

[28] P. Sivashanmugam, S. Suresh, Experimental studies on heat transfer and friction factor characteristics of laminar flow through a circular tube fitted with regularly spaced helical screw-tape inserts, Experimental Thermal and Fluid Science 31 (2007) 301-308.

[29] P. Sivashanmugam, S. Suresh, Experimental studies on heat transfer and friction factor characteristics of turbulent flow through a circular tube fitted with regularly spaced helical screw-tape inserts, Applied Thermal Engineering 27 (2007) 1311-1319.

[30] S.R. Krishna, G. Pathipaka, P. Sivashanmugam, Heat transfer and pressure drop studies in a circular tube fitted with straight full twist, Experimental Thermal and Fluid Science 33 (2009) 431-438.

[31] P. Sivashanmugam, P.K. Nagarajan, Studies on heat transfer and friction factor characteristics of laminar flow through a circular tube fitted with right and left helical screw-tape inserts, Experimental Thermal and Fluid Science 32 (2007) 192-197.

[32] P. Sivashanmugam, P.K. Nagarajan, S. Suresh, Experimental studies on heat transfer and friction factor characteristics in turbulent flow through a circular tube fitted with right-left helical screw-tape inserts, Chemical Engineering Communication 195 (2008) 977-987.

[33] S. Jaisankar, T.K. Radhakrishnan, K.N. Sheeba, Experimental studies on heat transfer and thermal performance characteristics of thermosyphon solar water heating system with helical and left-right twisted tapes, Energy Conversion and Management 52 (2011) 2048-2055.

[34] P.K. Nagarajan, Yagna Mukkamala, P. Sivashanmugam, Studies on heat transfer and friction factor characteristics of turbulent flow through a micro-finned tube fitted with left-right inserts, Applied Thermal Engineering, 30 (2010) 1666-1672.

[35] S. Jaisankar, T.K. Radhakrishnan, K.N. Sheeba, Experimental studies on heat transfer and friction factor characteristics of thermosyphon solar water heater system fitted with spacer at the trailing edge of twisted tapes, Applied Thermal Engineering 29 (2009)1224-1231.

This material is reserved for educational use only, not allowed for commercial use.
Forbidden to modify the content, and cite the document when use.

[36] P. Murugesan, K. Mayilsamy, S. Suresh, Turbulent heat transfer and pressure drop in tube fitted with square-cut twisted tape, Chinese Journal of Chemical Engineering 18, (2010) 609-617.

[37] P. Murugesan, K. Mayilsamy, S. Suresh, P.S.S. Srinivasan, Heat transfer and pressure drop characteristics in a circular tube fitted with and without V-cut twisted tape insert, International Communications in Heat and Mass Transfer 38 (2011) 329-334.

[38] P. Murugesan, K. Mayilsamy, S. Suresh, Heat transfer in tubes fitted with trapezoidal-cut and plain twisted tape inserts, Chemical Engineering Communications 198 (2011) 886-904.

[39] S.K. Saha, Thermohydraulics of laminar flow of viscous oil through a circular tube having axial corrugations and fitted with centre-cleared twisted tape, Experimental Thermal and Fluid Science 38 (2012) 201-209.

[40] S. K. Saha, S. Bhattacharyya, P. K. Pal, Thermohydraulics of laminar flow of viscous oil through a circular tube having integral axial rib roughness and fitted with center-cleared twisted tape, Experimental Thermal and Fluid 41 (2012) 121-129.

[41] S. Bhattacharyya, S.K. Saha, Thermohydraulics of laminar flow through a circular tube having integral helical rib roughness and fitted with centre-cleared twisted tape, Experimental Thermal and Fluid Science 42 (2012) 154-162.

[40] S.K. Saha, Thermohydraulics of turbulent flow through rectangular and square ducts with axial corrugation roughness and twisted-tapes with and without oblique teeth, Experimental Thermal and Fluid Science 34 (2010) 744-752.

[42] S. Eiamsa-ard, K. Nanan, C. Thianpong, P. Eiamsa-ard, Thermal performance evaluation of heat exchanger tubes equipped with coupling twisted-tapes, Experimental Heat Transfer: A Journal of Thermal Energy Generation, Transport, Storage, and Conversion 26 (2013) 413-430.

[43] S. Eiamsa-ard, C. Nuntadusit, P. Promvonge, Effect of twin delta-winged twisted-tape on thermal performance of heat exchanger tube, Heat Transfer Engineering, An International Journal, 34 (2013)1278-1288.

[44] S.W. Chang, K.W. Yu, M.H. Lu, Heat transfer in tubes fitted with single, twin and triple twisted tapes, Experimental Heat Transfer 18 (2005) 279-294.

[45] S. Eiamsa-ard, C. Thianpong, P. Eiamsa-ard, Turbulent heat transfer enhancement by counter/co-swirling flow in a tube fitted with twin twisted tapes, Experimental Thermal and Fluid Science 34 (2010) 53-62.

[46] S. Eiamsa-ard, C. Thianpong, P. Eiamsa-ard, P. Promvonge, Thermal characteristics in a heat exchanger tube fitted with dual twisted tape elements in tandem, International Communications in Heat and Mass Transfer 37 (2010) 39-46.

This material is reserved for educational use only, not allowed for commercial use.
Forbidden to modify the content, and cite the document when use.

[47] X. Zhang, Z. Liu, W. Liu, Numerical studies on heat transfer and flow characteristics for laminar flow in a tube with multiple regularly spaced twisted tapes, International Journal of Thermal Sciences 58 (2012) 157-167.

[48] Y. Hong, X. Deng, L. Zhang, 3D Numerical study on compound heat transfer enhancement of converging-diverging tubes equipped with twin twisted tapes, Chinese Journal of Chemical Engineering 20 (2012) 589-601.

[49] W. Duangthongsuk, S. Wongwises, An experimental study on the heat transfer performance and pressure drop of TiO_2-water nanofluids flowing under a turbulent flow regime, International Journal of Heat and Mass Transfer 53 (2010) 334-344.

[50] M.H. Kayhani, H. Soltanzadeh , M.M. Heyhat , M. Nazari, F. Kowsary, Experimental study of convective heat transfer and pressure drop of TiO_2/water nanofluid, International Communications in Heat and Mass Transfer 39 (2012) 456-462.

[51] A. Zamzamian, S.N. Oskouie, A. Doosthoseini, A. Joneidi,M. Pazouki, Experimental investigation of forced convective heat transfer coefficient in nanofluids of Al_2O_3/EG and CuO/EG in a double pipe and plate heat exchangers under turbulent flow, Experimental Thermal and Fluid Science 35 (2011) 495-502.

[52] P. Razi, M.A. Akhavan-Behabadi, M. Saeedinia, Pressure drop and thermal characteristics of CuO-base oil nanofluid laminar flow in flattened tubes under constant heat flux, International Communications in Heat and Mass Transfer 38 (2011) 964-971.

[53] K.V. Sharma, L. Syam Sundar, P.K. Sarma, Estimation of heat transfer coefficient and friction factor in the transition flow with low volume concentration of Al_2O_3 nanofluid flowing in a circular tube and with twisted tape insert, International Communications in Heat and Mass Transfer 36 (2009) 503-507.

[54] L. Syam Sundar, K.V. Sharma, Turbulent heat transfer and friction factor of Al_2O_3 nanofluid in circular tube with twisted tape inserts, International Communications in Heat and Mass Transfer 53 (2010) 1409-1416.

[55] L. Syam Sundar, N.T. Ravi Kumar, M.T. Naik, K.V. Sharma, Effect of full length twisted tape inserts on heat transfer and friction factor enhancement with F_e3O_4 magnetic nanofluid inside a plain tube: An experimental study, International Journal of Heat and Mass Transfer 55 (2012) 2761-2768.

[56] A.A. Abbasian Arani, J. Amani, Experimental study on the effect of TiO_2-water nanofluid on heat transfer and pressure drop, Experimental Thermal and Fluid Science 42 (2012) 107-115.

[57] K. Wongcharee, S. Eiamsa-ard, Enhancement of heat transfer using CuO/water nanofluid and twisted tape with alternate axis, International Communications in Heat and Mass Transfer 38 (2011) 742-748.

This material is reserved for educational use only, not allowed for commercial use.
Forbidden to modify the content, and cite the document when use.

[58] M.T. Naik, G. Ranga Janardana, L. Syam Sundar, Experimental investigation of heat transfer and friction factor with water-propylene glycol based CuO nanofluid in a tube with twisted tape inserts, International Communications in Heat and Mass Transfer 46 (2013) 13-21.

[59] ANSI/ASME, Measurement Uncertainty, PTC 19, 1-1985. Part I, 1986.

[60] B.C. Pak, Y.I. Cho, Hydrodynamic and heat transfer study of dispersed fluids with submicron metallic oxide particles, Experimental Heat Transfer 11 (1998) 151-170.

[61] Y. Xuan, W. Roetzel, Conceptions for heat transfer correlation of nanofluids, International Journal of Heat and Mass Transfer 43 (2000) 3701–3707.

[62] Maxwell, J.C., Treatise on Electricity and Magnetism, Dover, New York, 1954.

[63] M. Chandrasekar, S. Suresh, B.A. Chandra, Experimental studies on heat transfer and friction factor characteristics of Al_2O_3/water nanofluid in a circular pipe under laminar flow with wire coil inserts, Experimental Thermal and Fluid Science 34 (2010) 122-130.

[64] A. Einstein, Berichtigung zu meiner Arbeit: eine neue Bestimmung der Molekul- dimensionen, Annals of Physics 34 (1911) 591.

[65] F.P. Incropera, P.D. DeWitt, T.L. Bergman, A.S. Lavine, Fundamentals of Heat and Mass Transfer, John-Wiley & Sons, 2006.

[66] S.K. Saha, Thermohydraulics of turbulent flow through rectangular and square ducts with axial corrugation roughness and twisted-tapes with and without oblique teeth, Experimental Thermal and Fluid Science 34 (2010) 744-752.

[67] S.J. Kline, F.A. McClintock, Describing Uncertainties in Single Sample Experiments, Mechanical Engineering 75 (1953) 3-8.

King Mongkut's Institute of Technology Ladkrabang

This material is reserved for educational use only, not allowed for commercial use.
Forbidden to modify the content, and cite the document when use.

Appendix

Budget details

1. Expenses	10,000 Baht
2. Materials	30,000 Baht
3. Others	20,000 Baht

King Mongkut's Institute of Technology Ladkrabang

This material is reserved for educational use only, not allowed for commercial use.
Forbidden to modify the content, and cite the document when use.

Curriculum Vitae

Name Dr. Kunlanan Kiatkittipong

Position Lecturer

Education 2008: B.Sc. (Chem. Eng.), Chulalongkorn University, Thailand

2012: Ph.D. (Chem. Eng.), The University of New South Wales, Australia

Research area

- Developing and exploiting new nanostructured materials with controllable size and properties for energy and environmental applications;
- Approaching H_2 production for the future clean energy and degradation of pollutant in air and waste water through photocatalytic reaction over advanced functional nanomaterial;
- Approaching catalytic processes for alternative and renewable fuel productions from local feedstocks (e.g., biogas, natural gas, crude palm oil and lignocellulosic biomass);
- Enhancing thermal performance characteristics in a heat exchanger tube by using Ti-O based catalyst as the working fluid.

Honors, Awards and Scholarship

- Postgraduate Research Student Support Award
- Ph.D. Scholarship (Australian Research Council, ARC)
- Best Presentation at Chemeca Conference 2011
- Invited lecture "Advanced Functional Nanomaterials and their Applications" Department of Chemical Engineering, Faculty of Engineering and Industrial Technology, Silpakorn University (2012 and 2013).

Publications

1. Eiamsa-ard, S., **Kiatkittipong, K.**, (2014) Heat transfer enhancement by multiple twisted tape inserts and TiO_2/water nanofluid, *Applied Thermal Engineering* 70, 896-924 (impact factor 2013 = 2.624)
2. Pairojpiriyakul, T., Croiset, E., **Kiatkittipong, K.**, Kiatkittipong, W., Arpornwichanop, A., Assabumrungrat, S. (2014) Catalytic reforming of glycerol in supercritical water with nickel-based catalyst, *International Journal of Hydrogen Energy* 39 (27), 14739-14750. (impact factor 2013 = 2.930)
3. **กุลนันทน์ เกียรติกิตติพงษ์** (2013), การผลิตไฮโดรเจนโดยใช้ริบบอนนาโนไททาเนตโครงสร้างแบบชั้นที่แลกเปลี่ยนด้วยทิน (II) ไอออน ภายใต้แสงวิสิเบิล, *วารสารวิศวกรรมศาสตร์* 2, 1-12

This material is reserved for educational use only, not allowed for commercial use.
Forbidden to modify the content, and cite the document when use.

4. **กุลนันทน์ เกียรติกิตติพงษ์** (2013), การสังเคราะห์โครงสร้างระดับนาโนเมตรไททาเนตด้วยวิธีไฮโดรเทอร์มัล, *วารสารสมาคมวิศวกรรมเคมีและเคมีประยุกต์แห่งประเทศไทย* 3, 64-69.
5. Kiatkittipong, W., Phimsen, S., **Kiatkittipong, K.**, Wongsakulphasatch, S., Laosiripojana, N., Assabumrungrat, S. (2013) Diesel-like hydrocarbons production from hydroprocessing of relevant refining palm oil, *Fuel Processing Technology* 116, 16-26 (impact factor 2013 = 3.019)
6. Pairojpiriyakul, T., Croiset, E., Kiatkittipong, W., **Kiatkittipong, K.**, Arpornwichanop, A., Assabumrungrat, S. (2013) Hydrogen production from catalytic supercritical water reforming of glycerol with cobalt based catalysts, *International Journal of Hydrogen Energy* 38 (11), 4368-4379. (impact factor 2013 = 2.930)
7. **Kiatkittipong, K.**, Iwase, A., Scott, J., Amal, R. (2013) Photocatalysis of heat treated sodium- and hydrogen- titanate nanoribbons for water splitting, H_2/O_2 generation and oxalic acid oxidation, *Chemical Engineering Science*, 33, 341-349 (impact factor 2013 = 2.613)
8. **Kiatkittipong, K.**, Scott, J., Amal, R. (2011) Hydrothermally synthesised titanate nanostructures: Impact of heat treatment on particle characteristics and photocatalytic properties, *ACS Applied Materials & Interfaces,* 3, 3988-3996. (impact factor 2013 = 5.900)
9. **Kiatkittipong, K.,** Ye, C., Scott, J., Amal, R. (2010) Understanding hydrothermal titanate nanoribbon formation, *Crystal Growth & Design*, 10, 3618-3625. (impact factor 2013 = 4.558)
10. **Kiatkittipong, K.**, Ye, C., Scott, J., Amal, R (2010) Investigation preparation parameters during titanium oxide nanoribbon synthesis, *IEEE Explore* on Nanoscience and Nanotechnology, 6045196, 105-107.
11. Wang, Y., Chan S.L., Amal, R., Shen, Y.R., **Kiatkittipong, K.** (2010). XRD Anisotropic Broadening of Nano-Particles, *Powder Diffraction* 25, 217. (impact factor 2013 = 0.544)

Refereed International Conference Proceedings

1. **Kiatkittipong, K.**, Assabumrungrat, S. (2014) Understanding phase transformation of titanate nanoribbons by heat treatment, Proceedings, 23rd International Symposium on Chemical Reaction Engineering (ISCRE 23) and 7th Asia-Pasific Chemical Reaction Engineering Symposium (APCRE 7) (7 – 10 September 2014, Bangkok, Thailand)
2. Teerachaiyapat, T., **Kiatkittipong, K.,** Kiatkittipong, W., Assabumrungrat, S. (2014) Ti-O nanoribbon photocatalyst: the ion exchange process of co^{2+} intercalated in layered nanoribbons, Proceedings, 23rd International Symposium on Chemical Reaction Engineering (ISCRE 23) and 7th Asia-Pasific Chemical Reaction Engineering Symposium (APCRE 7) (7 – 10 September 2014, Bangkok, Thailand)

This material is reserved for educational use only, not allowed for commercial use.
Forbidden to modify the content, and cite the document when use.

3. Phimsen, S., Kiatkittipong, W., **Kiatkittipong, K.,** Yamada, H., Tagawa, T., Laosiripojana, N., Assabumrungrat, S. (2014) Oil extracted from spent coffee grounds for bio-hydrogenated diesel production, Proceedings, 23rd International Symposium on Chemical Reaction Engineering (ISCRE 23) and 7th Asia-Pasific Chemical Reaction Engineering Symposium (APCRE 7) (7 – 10 September 2014, Bangkok, Thailand)
4. Pongsiriyakul, K., Kiatkittipong, W., **Kiatkittipong, K.,** Wongsakulphasatch, S., Laosiripojana, N., Assabumrungrat, S. (2014) Hydrotreated vegetable oil production under synthesis gas, Proceedings, 23rd International Symposium on Chemical Reaction Engineering (ISCRE 23) and 7th Asia-Pasific Chemical Reaction Engineering Symposium (APCRE 7) (7 – 10 September 2014, Bangkok, Thailand)
5. **Kiatkittipong, K.**, Pongsiriyakul, K., Phimsen, S., Kiatkittipong, W., Wongsakulphasatch, S., Laosiripojana, N., Assabumrungrat, S. (2013) Hydrotreated biodiesel production from palm fatty acid distillate, Proceedings, The 5th Regional Conference on Chemical Engineering (7-8 February 2013, Pattaya, Thailand)
6. **Kiatkittipong, K.**, Scott, J., Amal, R., The impact of calcination on titanate nanostructure characteristics and their ensuing photocatalytic properties, Proceedings, The 16th International Conference on TiO_2 Photocatalysis Fundamentals and Applications (7-10 November 2011, San Diego, USA)
7. **Kiatkittipong, K.**, Scott, J., Amal, R., Titanate nanostructure phase transformation and its influence on photocatalytic activity, Proceedings, Chemeca Conference (18-21 September 2011, Sydney, Australia)
8. **Kiatkittipong, K.,** Scott, J., Amal, R., The structural transformation of hydrothermally synthesized titanate nanoribbons and nanotubes and photocatalytic activity, Proceedings, 22nd North American Catalysis Society Meeting (5-10 June 2011, Detroit, USA)
9. **Kiatkittipong, K.,** Scott, J., Amal, R., An investigation of titanate nanostructure and photodegradation, Proceedings, The 7th Annual Conference of the ARC centre of Excellence for Functional Nanomaterials (25-26 November 2010, Gold Coast, Australia)
10. **Kiatkittipong, K.,** Scott, J., Amal, R, The effect of calcination temperature on titanate nanoribbon structure and its photocatalytic activity, Proceedings, Chemeca Conference (26-29 September 2010, Adelaide, Australia)
11. **Kiatkittipong, K.,** Ye, C., Scott, J., Amal, R, Synthesis condition and post treatment effect on titanate nanoribbons, Proceedings, The 6th Annual Conference of the ARC centre of Excellence for Functional Nanomaterials (9-11 November 2009, Coffs Harbour, Australia)

This material is reserved for educational use only, not allowed for commercial use.
Forbidden to modify the content, and cite the document when use.